Minimal controller synthesis for a full-bridge buck inverter

Alessandro Mastronardi

Supervisors:

Prof. Mario Di Bernardo
Prof. Josep M. Olm

July 23, 2013

Contents

1 Abstract

The main objective of this research study is the control of a DC-AC full-bridge buck-based inverter through an extension of Model reference adaptive control (MRAC) strategy, in particular the Extended Minimal Controller Synthesis. This approach requires minimal knowledge of plant and disturbance parameters offering a good robustness even in presence of parameters variation, plant unmodeled nonlinearities and external disturbances.

The rejection of undesirable effects of sudden load changes and the ability to recover regular operation with a low transient error, in a short number of periods and the high robustness guarantee that high performance is kept when the control signal is injected through a PWM generator switching at realistic frequency.

2 Introduction

Most of dynamic systems show unknown or time-varying parameters resulting difficult to control unless the controller is on-line redesigned:

- Robot manipulation may involve the handling of loads with different sizes and weights.
- Automatic ship steering has to take into account water depth, ship load, wind and wave conditions.
- Process control involves a hard modeling process and parameter identification, and usually time-varying working conditions.
- Power systems may undergo large load variations.
- Aircraft dynamics depends on its altitude, speed and configuration, with a high range of parameter variation.

2.1 Adaptive control

Adaptive control was first proposed in aerospace engineering early 1950âs in order to keep a consistent performance of the system in the face of uncertainty or variation in the plant parameters. The main feature was the adaptation of the controller gains on-line according to the variation of certain system signal.

The basics stages in adaptive control are:

- estimation of the unknown plant parameters
- updating of the control gains.

The main approaches of this kind of control are:

- Self-tuning controllers Model reference adaptive control.
- Model-Reference Adaptive Control

2.2 MRAC and MCS

he general idea behind Model Reference Adaptive Control (MRAC, also know as an MRAS or Model Reference Adaptive System) is to create a closed loop controller with parameters that can be updated to change the response of the system. The output of the system is compared to a desired response from a reference model. The control parameters are update based on this error. The goal is for the parameters to converge to ideal values that cause the plant response to match the response of the reference model.

The minimal control synthesis was proposed by Stoten Benchoubane in 1992, it is a passivity based MRAC strategy [8] which, for a wide class of plant structure, requires no knowledge of parameter values in order to achieve a stable and robust control performance. In addition, no a priori values for the controller gains are required,they are often set to zero, and no self-tuning component is necessary.

The key assumption of the MCS are:

- the system matrix $A(t)$,B have known dimensions and are in canonical form.
- The sign of b is known.
- The plant parameters vary slowly with respect to the adaptive gains.
- The gains are nonlinear and of PI type.
- The real constant $\alpha and \beta are chosen empirically. the strategy can be extended to MIMO plants.$

3 Overview of the Minimal Control Synthesis Algorithm

The MCS algorithm [4][5] is derived from a general MRAC[8] algorithm. Adaptive control provides capabilities that can be used to counteract the effect of dynamic changes and parameter variations. MRAC needs a good degree of knowledge of the nominal plant dynamics but this is not the case with MCS. The former must use some form of system identification in order to adapt the gains of the controller. MCS, on the other hand, does not require any parametric information and can start with zero gains. The main characteristics of MCS are:

- * No knowledge of the plant dynamic parameters is necessary.
  * The stability and robustness of the algorithm have been formally proved and tested.
  * The algorithm can cope with parameter variations and external disturbances as well as non-linear regimes.
  * It offers a high speed of response to disturbances.
  * The adaptive gains can be started from zero or be given an initial value to speed up convergence.
  * The adaptive gains can be locked transforming the algorithm into a virtual fixed-gain controller with automatic tuning.

* A linear controller can be used in parallel, allowing the algorithm to be implemented as a retrofit to an existing controller.

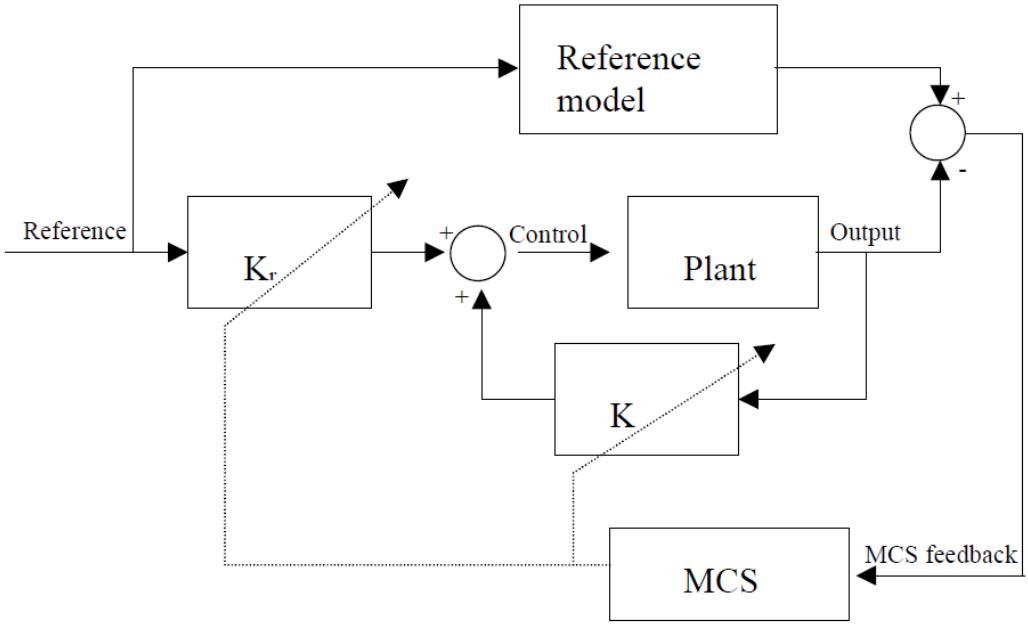

Figure 1: Block diagram of MCS

A block diagram of the algorithm is depicted in figure 1. The demand signal is modified by a reference model that produces the ideal close loop response. This response is compared to the output of the plant and the adaptive gains are modified in order to achieve a good matching between the output of the plant and the output of the reference model. The voltage bias usually present in analog devices can be removed using a third gain, which is computed based on the integral of the plant output error. This is known as the integral action (MCSIA) version and is described in [7].

3.1 The Minimal Control Synthesis algorithm

The standard MCS allow to control an n state system modeled by:

$$\dot{x}(t) = Ax(t) + Br(t) + d(x,t), \tag{1}$$

where u is the scalar control input and:

$$A = \begin{bmatrix} 0 & 1 & 0 & \dots & 0 \\ 0 & 0 & 1 & 0 & 0 \\ \vdots & \vdots & \vdots & \vdots & \vdots \\ 0 & 0 & 0 & 0 & 1 \\ -a_1 & -a_2 & \dots & \dots & -a_n \end{bmatrix}; B = \begin{bmatrix} 0 \\ 0 \\ \vdots \\ 0 \\ b \end{bmatrix}; d(x,t) = \begin{bmatrix} 0 \\ \vdots \\ 0 \\ d_1 \end{bmatrix},$$

the matrix A and B are supposed completely unknown with the assumption of a slow variation in comparison with the adaptive loop bandwidth; the canonical structure of A and B is a key assumption of MCS . The term d_1 represents all the effects of external disturbances, unmodeled nonlinearities and plant parameter variation.

The control signal is:

$$u(t) = L_x(t)x(t) + L_r(t)r(t);$$

the adaptive gains are:

$$L_r(t) = \alpha \int_0^t y_e(\tau)x^T(\tau)\, d\tau + \beta y_e(t)x^T(t),$$

$$L_x(t) = \alpha \int_0^t y_e(\tau)r(\tau)\, d\tau + \beta y_e(t)r(t),$$

where α and β are scalar adaption weights such that $sign(\alpha) = sign(\beta) = sign(b)$ and the initial conditions are usually set to zero.

The output error is:

$$x_e(t) = x_m(t) - x(t) \tag{2}$$

where x_m is the state generated by a linear reference model:

$$\dot{x}_m = A_m x_m(t) + B_m r(t)$$
$$y_e(t) = C_e x_e(t)$$

the output error matrix C_e is determined from positive-definite solution of Lyapunov equation:

$$PA_m + A_m^T P = -Q \quad ; Q > 0$$

as:

$$C_e = B_e^T P; B_e^T = [0 \ \dots \ 0 \ 1]$$

the structure of A_m and B_m is chosen to be the same of the plant:

$$A_m = \begin{bmatrix} 0 & 1 & 0 & \dots & 0 \\ 0 & 0 & 1 & 0 & 0 \\ \vdots & \vdots & \vdots & \vdots & \vdots \\ 0 & 0 & 0 & 0 & 1 \\ -a_m 1 & -a_m 2 & \dots & \dots & -a_m n \end{bmatrix}; B_m = \begin{bmatrix} 0 \\ 0 \\ \vdots \\ 0 \\ b_m \end{bmatrix}$$

A,B and $r(t)$ are selected by design in order to obtain:

$$\lim_{t \to \infty} x_e(t) = 0$$

3.2 The Extended Minimal Control Synthesis algorithm

The asymptotic stability of the error dynamics is not guaranteed if the term d(x,t) represents rapidly varying disturbances. The EMCS introduces an additional sliding action to achieve global asymptotic stability of the error dynamics under that conditions [3]. The control equation is:

$$u(t) = L_x(t)x(t) + L_r(t)r(t) + Nsign(y_e).$$

The gain L_x and L_r are chosen in the same way of the standard MCS algorithm. The N gain determines the amplitude of the switching action of the new control action term. The choice of a suitable value for the N gain requires a minimum knowledge of the system and in particular an estimate for b and the upper bound of the external disturbance d_1; this is against the philosophy of the MCS algorithm. To overcome the standard EMCS limitation according with [2] is possible to set the N gain in adaptive way getting a purely adaptive algorithm described by the control law :

$$u(t) = L_x(t)r(t) + L_r(t)r(t) + K_N(t)sgn(y_e(t))$$

where:

$$K_N(t) = \int_0^t \gamma \left|y_e(\tau)\right| \, d\tau, \quad K_N(0) = 0,$$

with $\gamma > 0$ being a positive adaptive weight. The presence of the *sign* function involves high frequency discontinuity, which implies that the control signal undergoes chattering phenomena provoking undesirable oscillations of the plant states. The use of such a control signal might excite the plant high frequency dynamics and initiate closed-loop instability. The robustness properties are preserved using the following continuous law:

$$u(t) = L_x(t)r(t) + L_r(t)r(t) + N\frac{y_e}{|y_e| + \xi}$$

where ξ is a small positive constant chosen according to 2.

3.3 Discrete-time version

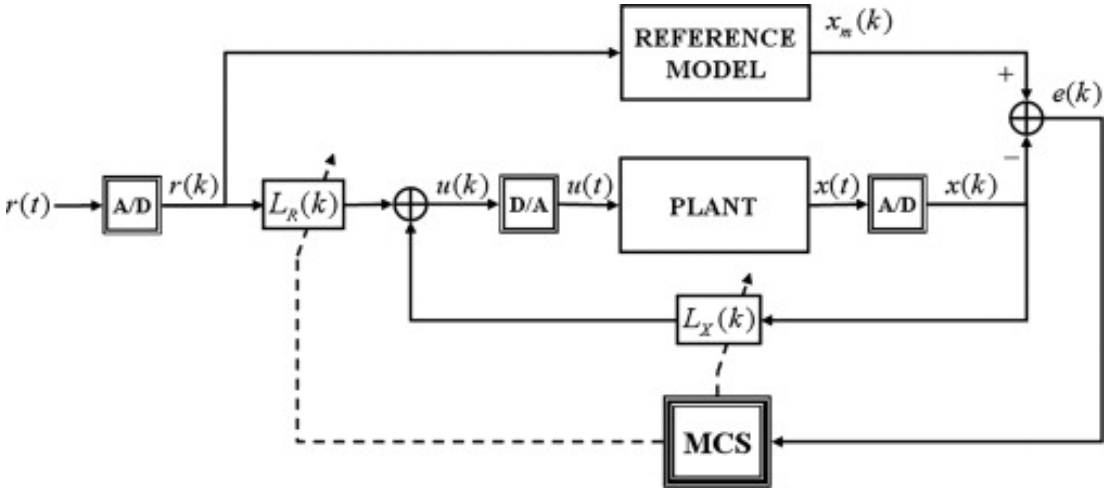

Figure 2: Block diagram of discrete MCS

A pure discrete-time version is given in [7], as it happens with the continuous-time MCS strategy, the algorithm arises from the family of hyperstability-based discrete-time model reference adaptive controllers introduced in [8] and is able to ensure tracking of the states of a given reference model with minimal knowledge about plant. The discrete-version grants the same advantages of the continuous algorithm. Also in [7] is shown a discrete-time MCS algorithm that can be used to control discretised continuous-time plants with the same performance features; this particular version is explicated below. Applying a forward Eulers's method with sampling period $T_s \in \mathbb{R}^+$[1] it is possible to discretize (1)-(2),obtaining:

$$x(k+1) = \mathbb{I}_n + T_s A(k) + T_s B b u(k),$$

$$x_m(k+1) = \mathbb{I}_n + T_s A_m(k) + T_s B b_m r(k).$$

Defining the state tracking error as $e(k) = x_m(k) - x(k)$, the control objective can be easily summarized as demanding

$$\lim_{k\to\infty} e(k) = \lim_{k\to\infty} \|x_m(k) - x(k)\| = 0$$

The control problem can be solved by the following discrete-time law composed by a feedback and a feedforward action:

$$u(k) = L_x(k)x(k) + L_r(k)r(k),$$

where $L_x(k) \in \mathbb{R}$ and $L_r(k) \in \mathbb{R}$ are adaptive gains of the form:

$$L_x(k) = \alpha \sum_{0}^{t} y_n(i+1)x^T(i) + \beta y_n(k+1)x^T(k),$$

$$L_r(k) = \alpha \sum_{0}^{t} y_n(i+1)r(i) + \beta y_n(k+1)r(k),$$

with $y(k)$ being a conveniently selected system output,$y_n(\cdot)$ being the n-th component of $y(\cdot)$ and α, $\beta \in \mathbb{R}$ being some constant values verifing $sign(\alpha) = sign(\beta) = sign(b)$. The control scheme is sketched in fig.2. The dynamics of the equivalent error system is:

$$e(k+1) = \widetilde{A}_m e(k) + \mathbb{I}_n \widetilde{\omega}(k+1),$$

$$y(k) = \widetilde{C} e(k),$$

where $\mathbb{I}_n$ denotes $n \times n$ identity matrix and

$$\widetilde{A}_m = \mathbb{I}_n + T_s A_m,$$

$$\widetilde{\omega}(k+1) = T_s \omega(k+1)$$

while

$$w(k+1) = \left[A_m - A(k) - BbL_x(k)\right] x(k) + B\left[b_m - bL_R(k)\right] r(k).$$

The computation of the control gains at the current instant k is based on the knowledge of the value reached by the plant output at the next time instant, namely $y_n(k+1)$. This one-delay problem can be solved by means of an estimate of $y_n(k+1)$, say $y_n^0(k+1)$. Assuming:

$$y_n(k+1) = y_n^0(k+1)1 + T_s \widetilde{c}_{nn} b(\alpha+\beta)(x^T(k)x(k) + r^2(k)),$$

where $\widetilde{c}_{nn}$ is the (n,n) elements of the output matrix C.
The computation of $y_n^0(k+1)$ requires a perfect knowledge of $A(k)$ and is in contradiction with the MCS philosophy, for this reason it is replaced by $y_n(k)$. Notice that the computation of $y_n(k+1)$ requires the knowledge of the uncertain plant parameter b, this is replaced by a value falling within its range of variation, which is assumed to be know.

4 The full-bridge buck power converter parameter

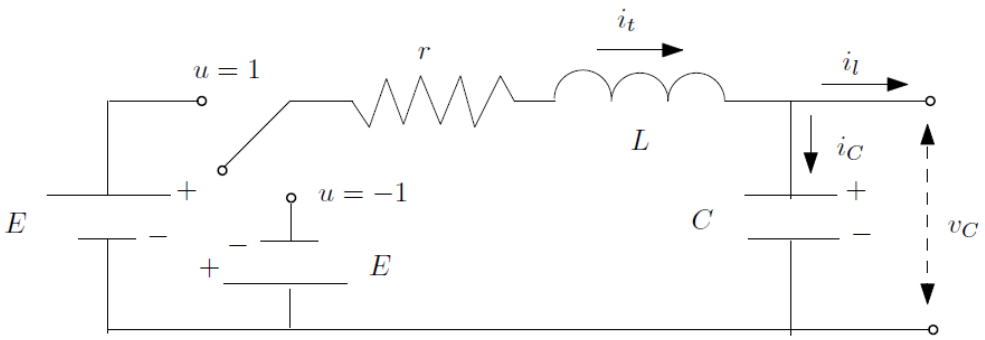

Figure 3: buck inverter

The mathematical model of the buck converter can be easily obtained under the common assumption of ideal components, the dynamic behavior of the full-bridge buck inverter can be described exploiting the Kirchhoff's equations:

$$i_t = i_l + i_c$$

$$Eu = ri_t + L\frac{di_t}{dt} + v_c \quad u \in \{-1, 1\}$$

$$i_c = C\frac{dv_c}{dt}$$

Setting v_c and $\frac{dv_c}{dt}$ as state variables, respectively x_1 e x_2 and consider the change of variables:

$$x_1 = \frac{v_c}{E},\ x_2 = \frac{dx_1}{dt},\ t = \frac{1}{\sqrt{LC}}\tau,\ \lambda_r = r\sqrt{\frac{C}{L}},\ \xi_l = \frac{1}{E}\sqrt{\frac{L}{C}}i_l$$

the dynamic model with normalized variables is:

$$\dot{x_1} = x_2$$

$$\dot{x_2} = -x_1 - \lambda_r x_2 + u - \lambda_r \xi_l - \dot{\xi}_l$$

for a linear load $i_l = \frac{v_c}{R}$ the model obtained will be the following:

$$\dot{x}_1 = x_2$$

$$\dot{x}_2 = \frac{E}{LC}u - \frac{R+r}{RLC}x_1 - \frac{rRC+L}{RLC}x_2$$

5 Simulation settings

The control goal is to have the converter voltage, $V_c(t)$, robustly tracking a sinusoidal reference profile, $V_{cd}(t)$ where

$$V_{cd}(t) = Msin2\pi\nu t = Msin\omega t$$

in the face of sudden changes of load parameter,R.
The reference model is selected as a second order linear model, according to [1] i.e. of the form

$$\dot{V}_{cd} = \widehat{A}_m V_{cd} + B\widehat{r}(t)$$

so as to steer the dynamics of the inverter in the desired way where

$$\widehat{A}_m = \begin{bmatrix} 0 & 1 \\ -\omega^2 & -\frac{2k}{\sqrt{LC}} \end{bmatrix} \quad \widehat{r}(t) = \frac{2Mk\omega}{\sqrt{LC}} cos\omega t$$

with initial condition $V_{cd}(0) = (0, M\omega^2)$.

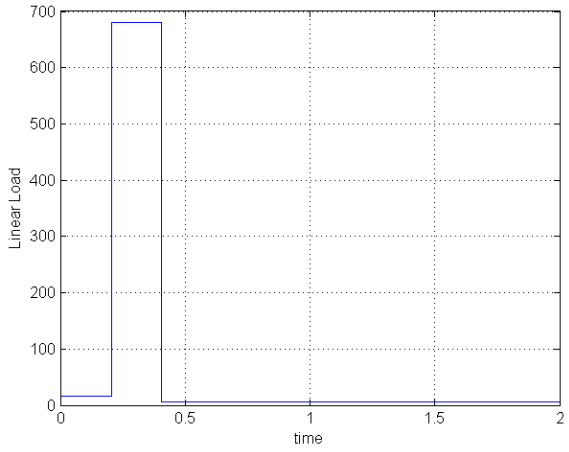

Figure 4: Output load resistance profile

The specific value for the reference profile are $M = 312V$ and $\nu = 50Hz$ which means that the expected output voltage should show European line frequency and $220V$ of Root Main Square (RMS) voltage. The high values of the parameters and signals involved suggest to carry out the control law implementation through normalized variables and, after validating the effectiveness proceed with the implementation in a denormalized fashion. α and β have been chosen heuristically as a trade off between convergence time and reactivity as suggest by the empirical rule $\frac{\alpha}{\beta} = 10$ according to [4]
The following simulations have been carried out with MATLAB-SIMULINK software. The solver uses a variable step ode45 algorithm or a fixed step algorithm ode4, depending of the cases, with minimum step size set to 10^-7. The controller performance in the face of load uncertainty has been assessed for the profile shown in fig.4: from $t = 0$ to $t = 0.205s$

the load was set to $R = 17\Omega$;at $t = 0.205s$ its value has been changed to $R = 680\Omega$,and at $t = 0.405s$ it has bean newly set to $R = 6.8\Omega$; The total duration for the test was of $2s$

6 Closed loop MCS on normalized buck dynamic model

the converter parameters for this simulation are:
$E = 220V$, $L = 6mH$, $C = 100$, $r = 0.2\Omega$, $R = 34\Omega$
, the expected output voltage is: $v_c d(\tau) = 220sin(100\pi\tau), \nu = 50Hz$,
in normalized variables it is: $x_1 d(t) = sin\omega_0 t$ with $\omega_0 = 100\pi\sqrt{LC}$,
the selected reference model is:

$$A_m = \begin{bmatrix} 0 & 1 \\ -\omega_0^2 & -2k \end{bmatrix}, \quad b_m = 1, \quad \text{r(t)=2k}\omega_0 cos(\omega_0 t)$$

the MCS controller gains are set to: $\alpha = 50, \beta = 5$,
the initial conditions for the plant are :$x_1(0) = 0.5, x_2(0) = 0$,
the initial conditions for the reference model are :$x_1(0) = 0,\ x_2(0) = \omega_0$.
The simulation results are the following:

6.1 Linear dynamic model

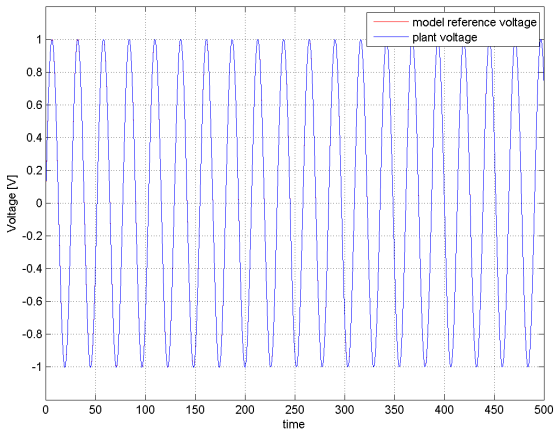

Figure 5: Output voltage evolution

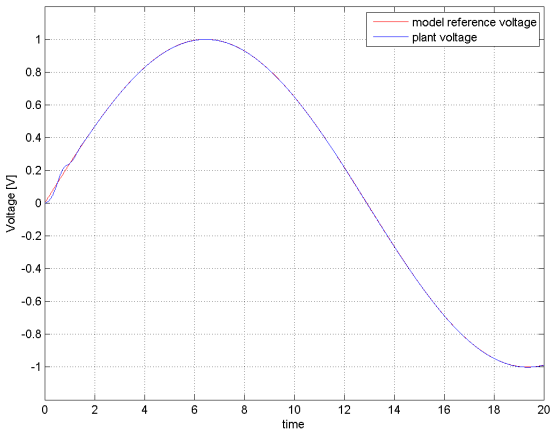

Figure 6: A zoom of the output voltage

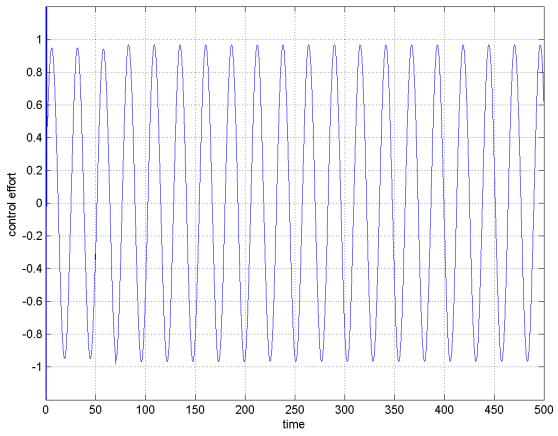

Figure 11: Control effort evolution

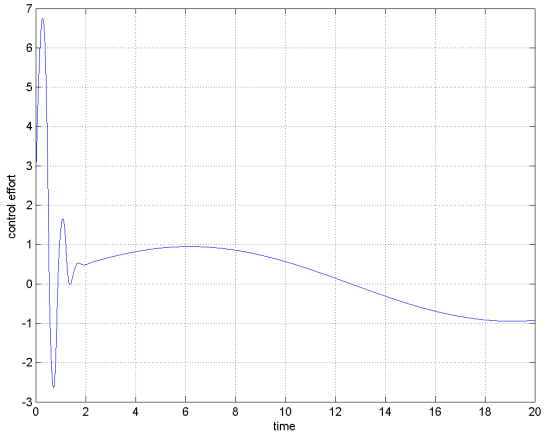

Figure 12: A zoom of the control effort

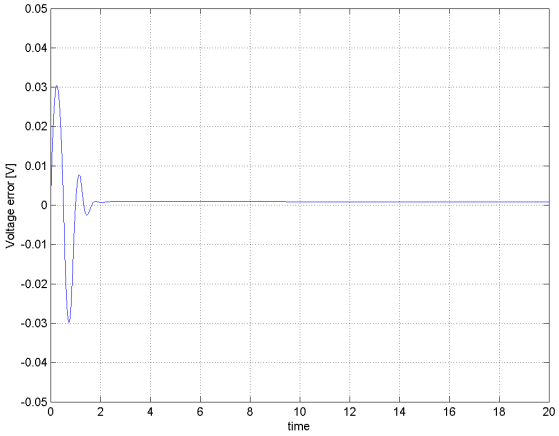

Figure 7: Error transient magnification

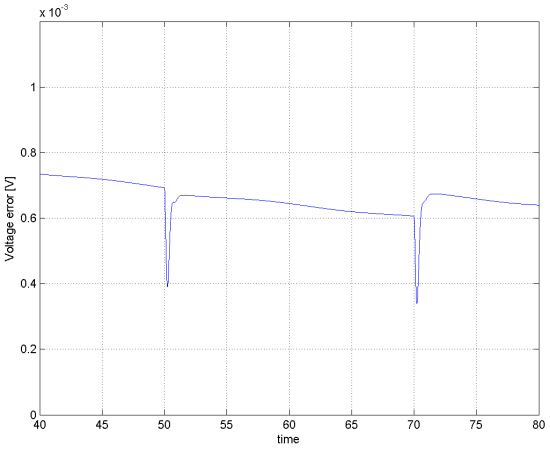

Figure 8: A zoom of the voltage tracking error

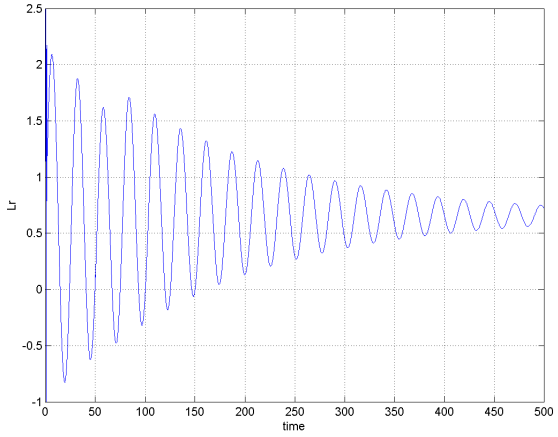

Figure 9: Lr gain evolution

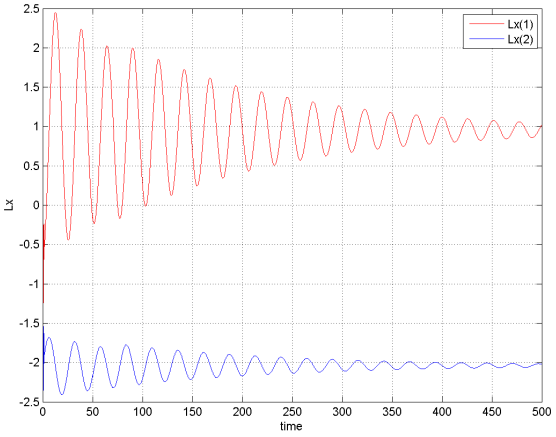

Figure 10: Lx gain trajectory

6.2 Nonlinear dynamic model

The shape of the nonlinear current i_l is the following:

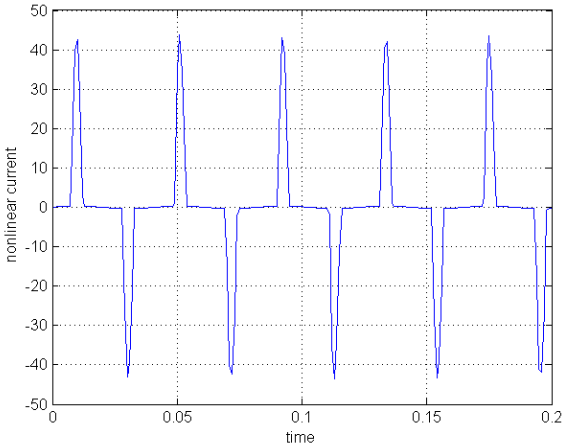

Figure 13: Nonlinear current shape

The results of simulation are:

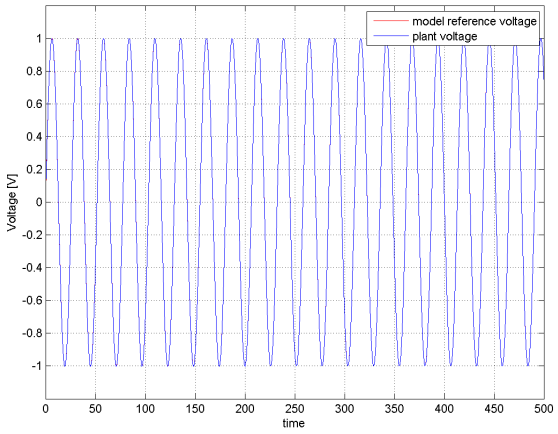

Figure 14: Output voltage evolution

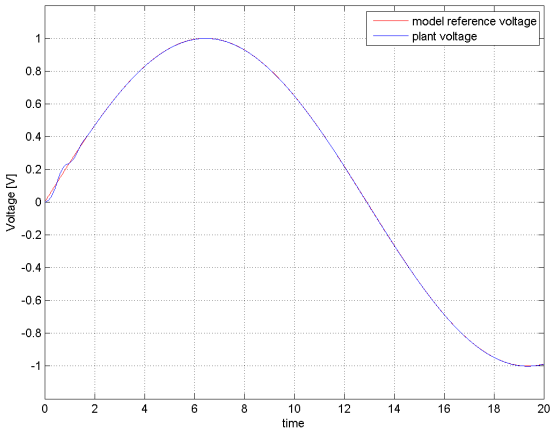

Figure 15: Output voltage transient zoom

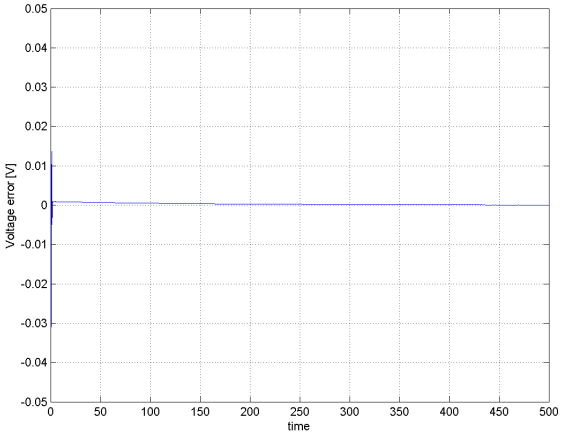

Figure 16: Voltage error trajectory

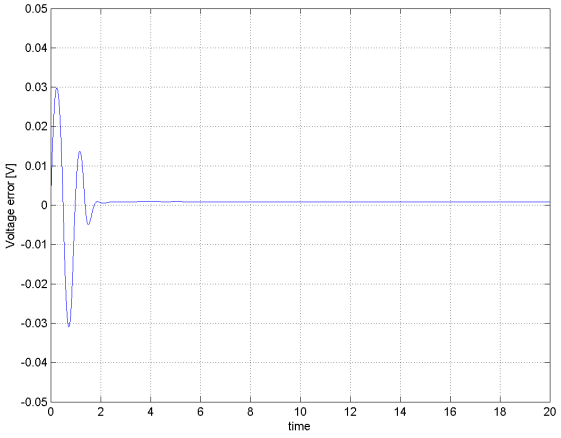

Figure 17: Zoom of error trajectory transient

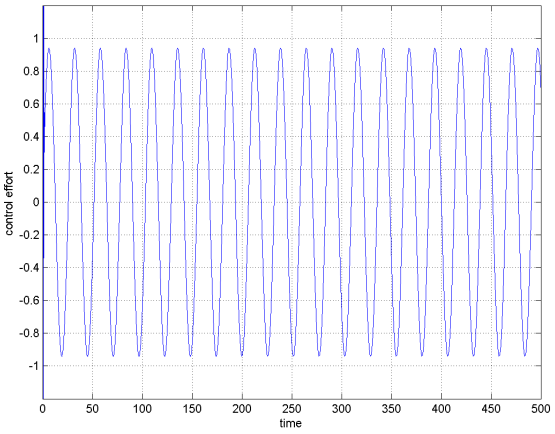

Figure 18: Control effort trajectory

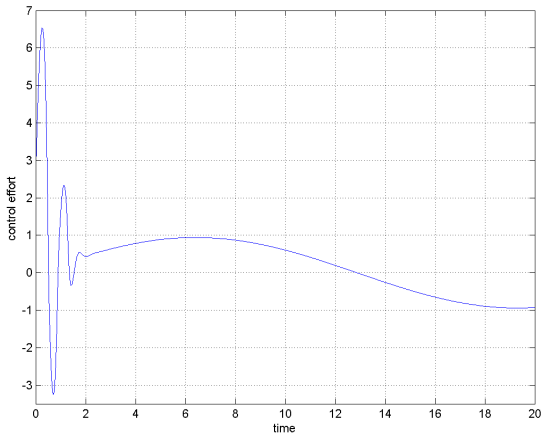

Figure 19: A zoom of control effort trajectory

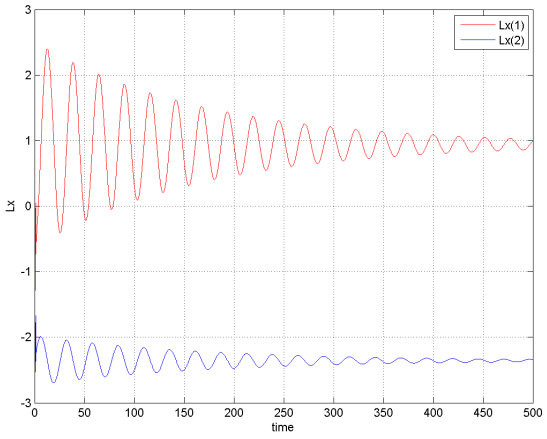

Figure 20: Lx gains trajectories

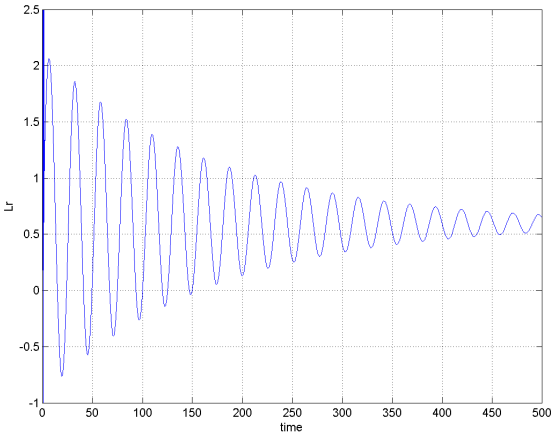

Figure 21: Lr dynamic

6.3 Results

The simulation shown consistent results as expected, the tracking of the reference signal is almost perfect as depicted in figure 5. A magnification of the very short transient is given in fig.6. The tracking error is depicted in fig.7, and a zoomed portray in fig.8, the maximum error is of 3% and is showed at very first time instants of the simulation as expected when the adaption process is just started, from that point it decays drastically towards zero. In fig.8 it is possible appreciate the recovery of the steady state error value in the face of a large load jump. The MCS gain evolution is shown in fig.9 and fig.10, where the response is the typical adaptive behavior. The control effort is given in fig.11 and fig.12, notice that never saturated but is kept in the bandwidth ± 1. For the Nonlinear load current depicted in fig.13 the results are almost the same as shown from fig.14 to fig.21.

7 Closed loop MCS on denormalized buck dynamic model

The converter parameters for this simulation are:
$E = 400V$, $L = 6mH$, $C = 10$, $r = 0.2\Omega$, $R = 34\Omega$,
the expected output voltage is: $v_c d(\tau) = 320sin(100\pi\tau), \nu = 50Hz$, $\omega_0 = 100\pi$
, the selected reference model is:

$$A_m = \begin{bmatrix} 0 & 1 \\ -\omega_0^2 & \frac{-2k}{\sqrt{LC}} \end{bmatrix}, b_m = 1, r(t) = 2k\omega_0 cos(\omega_0 t)$$

the MCS controller gains are set to: $\alpha = 2.5 \times 10^6$, $\beta = 2.5 \times 10^5$,
the initial conditions for the plant are :$x_1(0) = 0.5,\ x_2(0) = 0$,
the initial conditions for the reference model are :$x_1(0) = 0,\ x_2(0) = 312\omega_0$.
The simulation results are the following:

7.1 Linear dynamic model

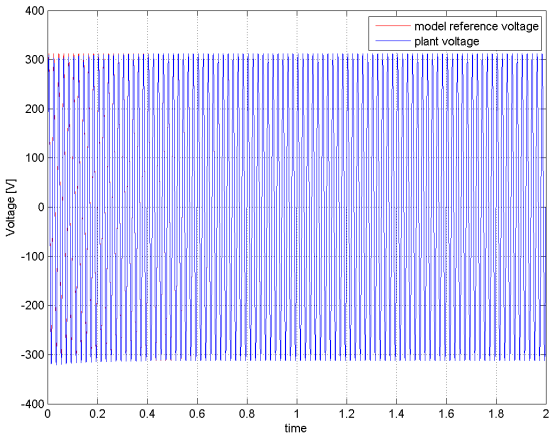

Figure 22: Voltage output evolution

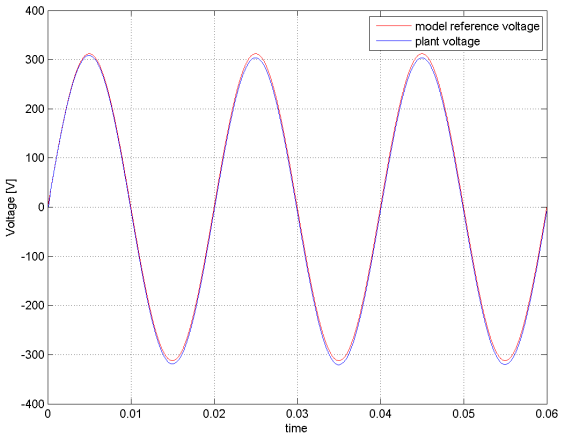

Figure 23: A zoom of the voltage evolution

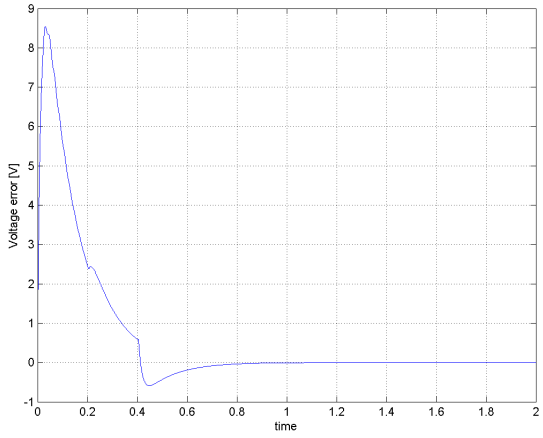

Figure 24: Voltage error evolution

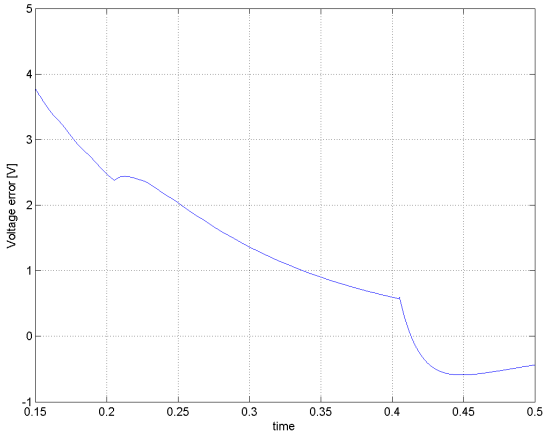

Figure 25: A zoom of error trajectory

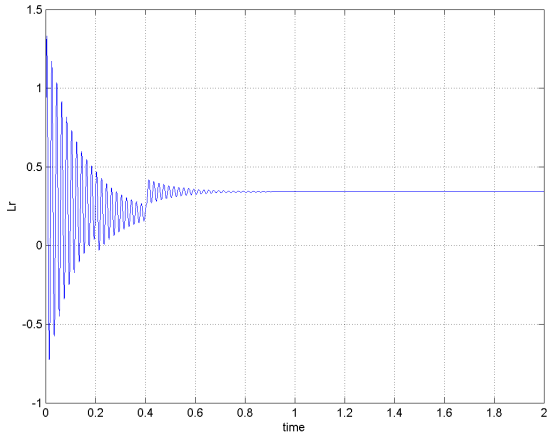

Figure 26: Lr gain evolution

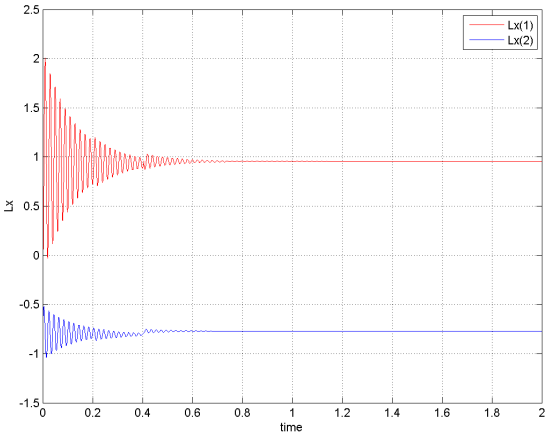

Figure 27: Lx gain trajectory

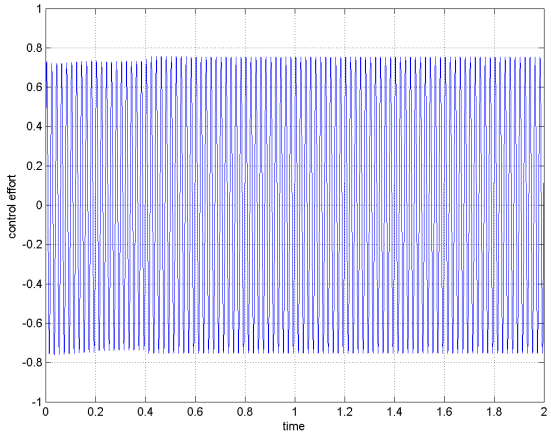

Figure 28: Control effort evolution

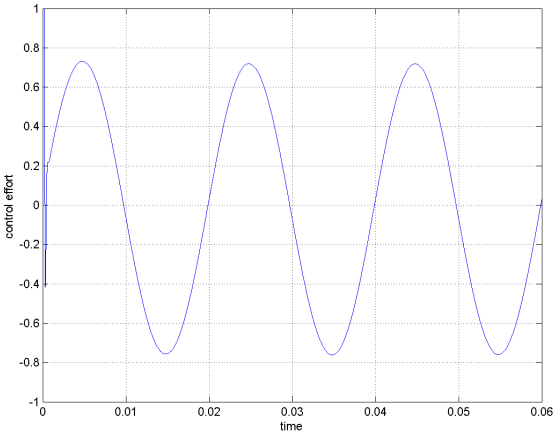

Figure 29: Control action magnification

7.2 Non linear dynamic model

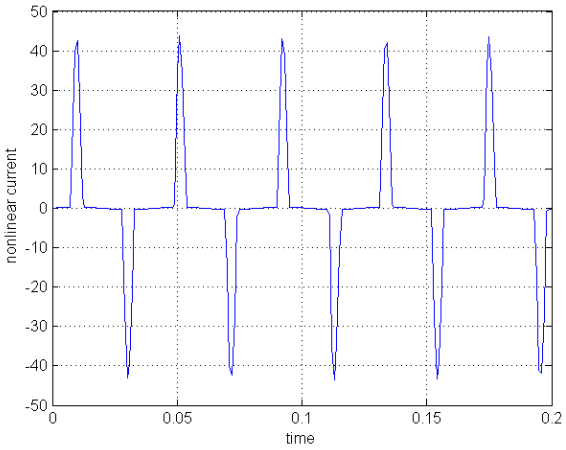

Figure 30: Nonlinear current shape

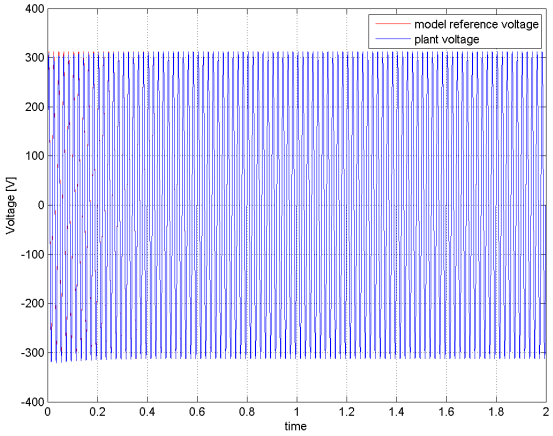

Figure 31: Output voltage evolution

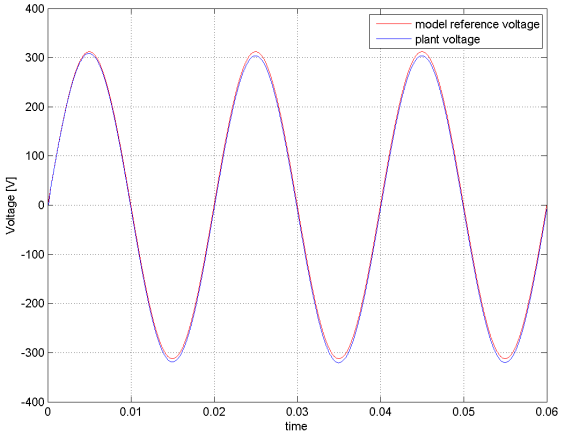

Figure 32: Output voltage transient

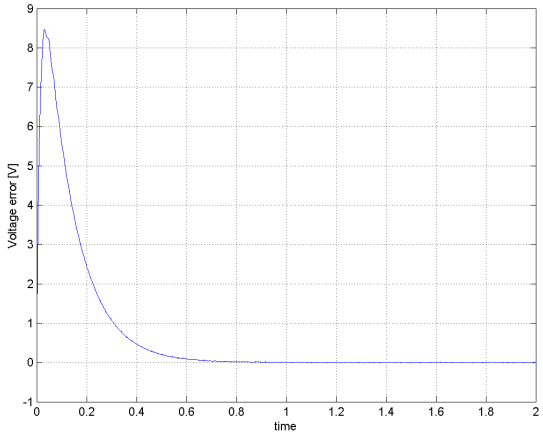

Figure 33: Voltage error dynamic

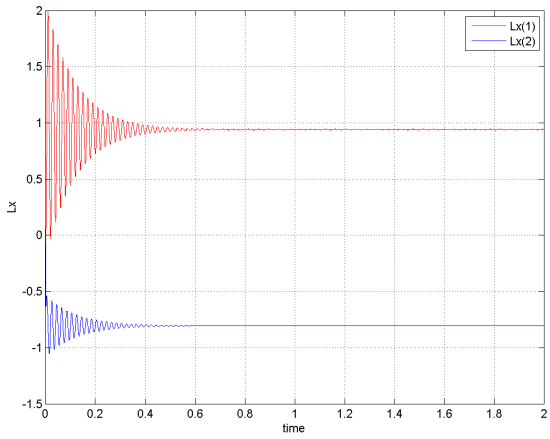

Figure 34: Lx gain evolution trajectories

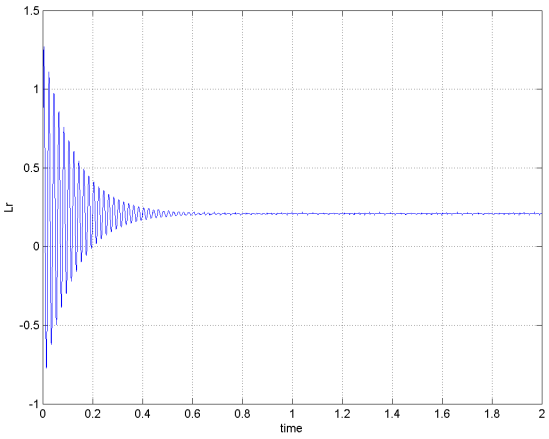

Figure 35: Lr gain trajectory

7.3 Results

The results obtained after the denormalization of the variables are satisfactory and consistent with the expected ones. In fig.22 it is possible realize the perfect tracking offered after the steady state is reached; a magnification of the transient, longer than the previous case, is given in fig.23. The maximum error is showed in fig.24: it is about 2.5% and it appear in the very first time instants of the simulation, then it decays dramatically toward zero. In fig.25 are highlighted the effects of the load variation to show the recovery capabilities of the MCS algorithm. The control effort is given in fig.28 and fig.29: notice that it never saturated,as desired. The MCS gain evolution is shown in fig.26 and fig.27, where it is evident the adaptation in the face of the load change. For the Nonlinear load depicted in fig.30 the results are almost the same as shown from fig. 31 to fig. 35 confirming the confirming the extraordinary robustness of the control algorithm.

8 Closed loop EMCS on denormalized power converter model

The converter parameters for this simulation are:
$E = 400V$, $L = 60$, $C = 40$, $r = 0.2\Omega$, $R = 17\Omega$, $k = 2$,
the expected output voltage is: $v_c d(\tau) = 320sin(100\pi\tau), \nu = 50Hz$, $\omega_0 = 100\pi$,
the reference model parameters and the initial conditions are the same setted in the precedent simulation the MCS controller gains are set to: $\alpha = 2.5 \times 10^{10}$, $\beta = 2.5 \times 10^{9}$.

8.1 Linear dynamic model

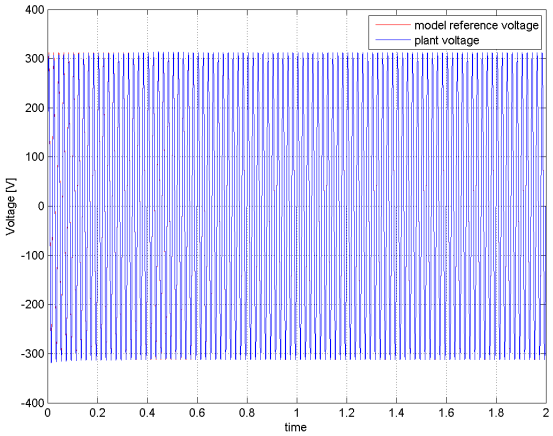

Figure 36: output voltage

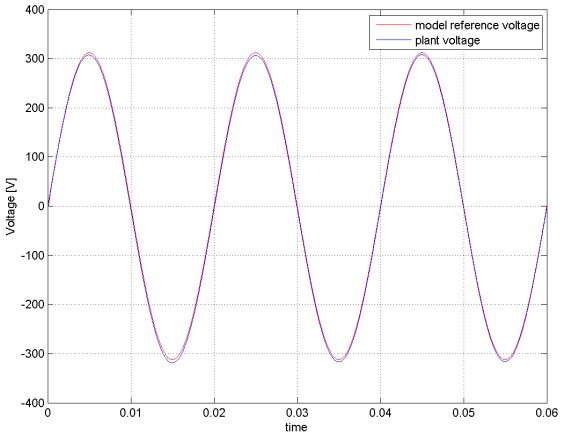

Figure 37: A zoom of the voltage evolution

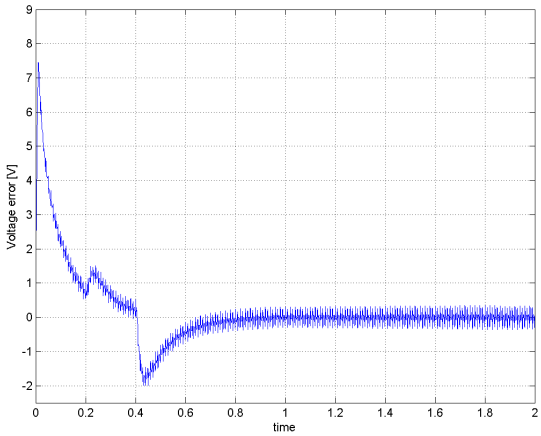

Figure 38: Voltage error dynamic

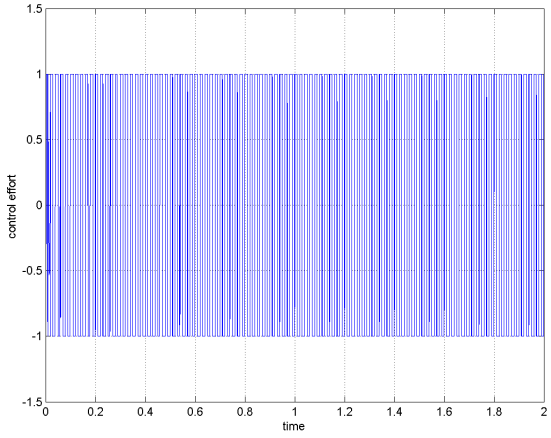

Figure 39: Control effort dynamic

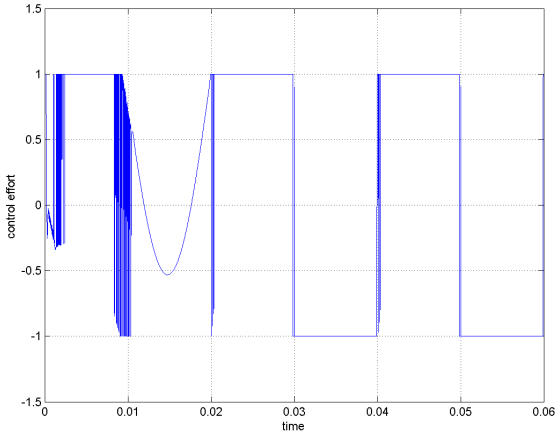

Figure 40: A zoom of the control effort

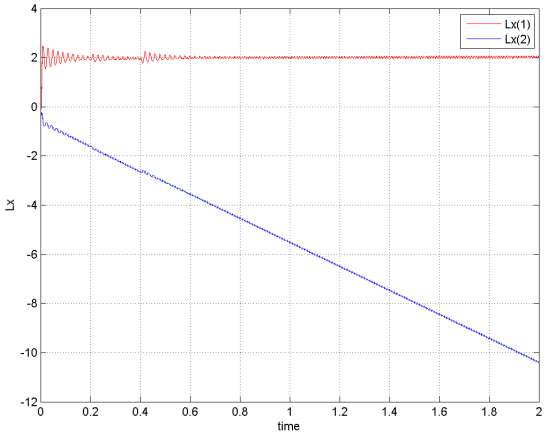

Figure 41: Lx gain dynamics

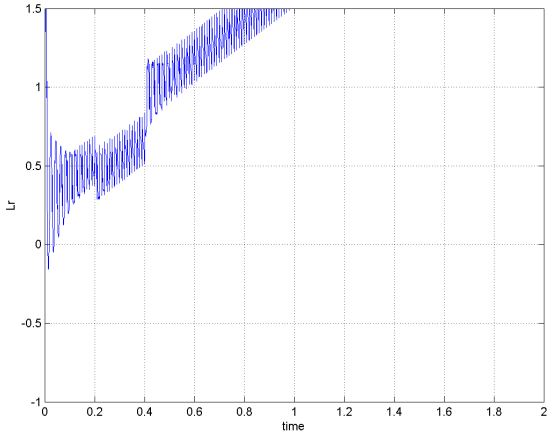

Figure 42: Lr gain evolution

Choosing the N gain in adaptive way:

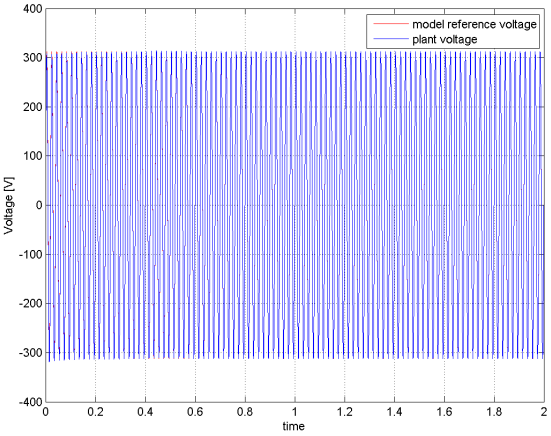

Figure 43: output voltage

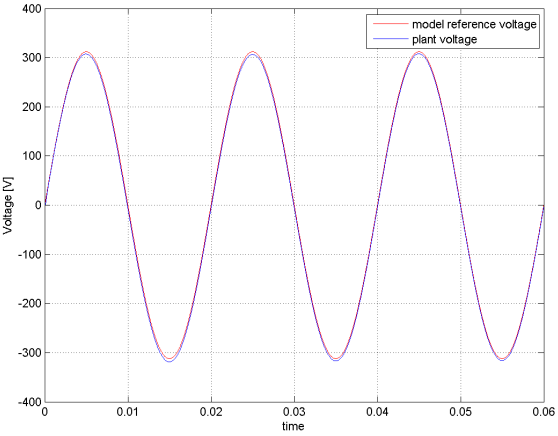

Figure 44: A zoom of the voltage evolution

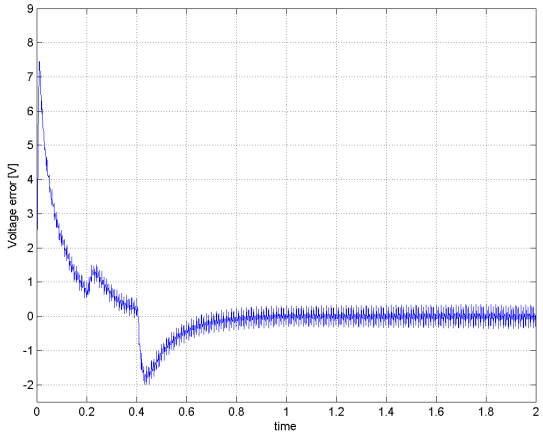

Figure 45: Voltage error dynamic

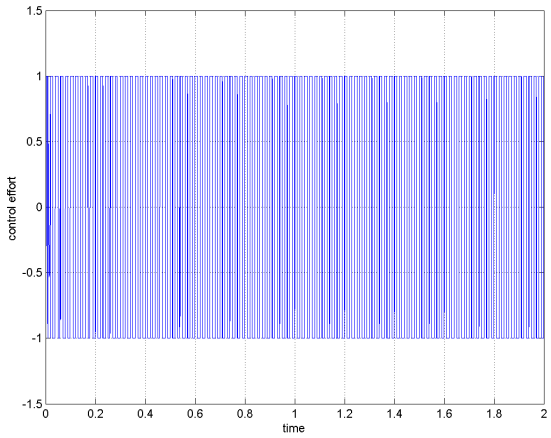

Figure 46: Control effort dynamic

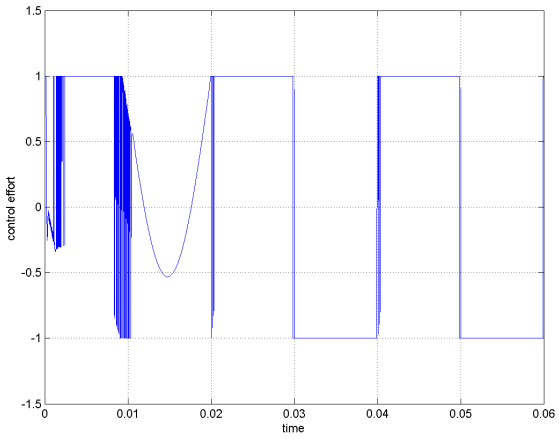

Figure 47: A zoom of the control effort trajectory

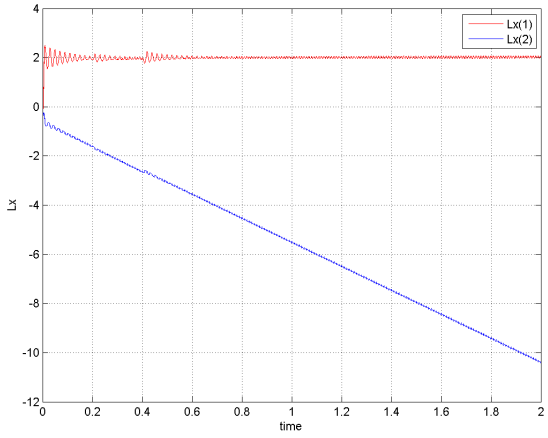

Figure 48: Lx gain dynamics

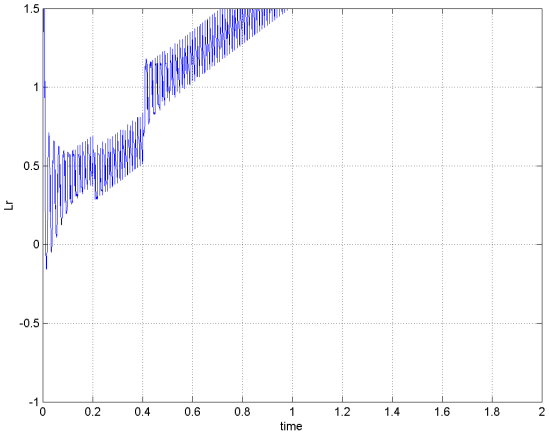

Figure 49: Lr gain evolution

Modeling the sliding action with a continuous law:

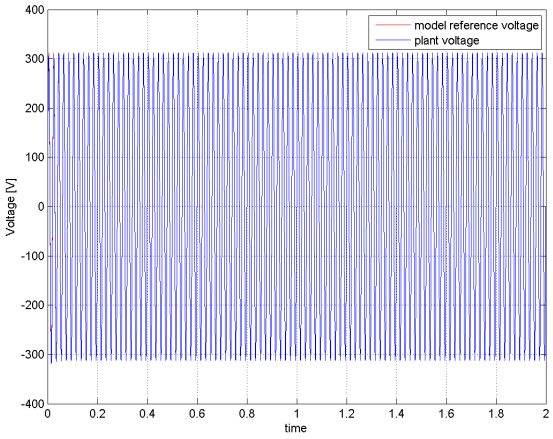

Figure 50: output voltage

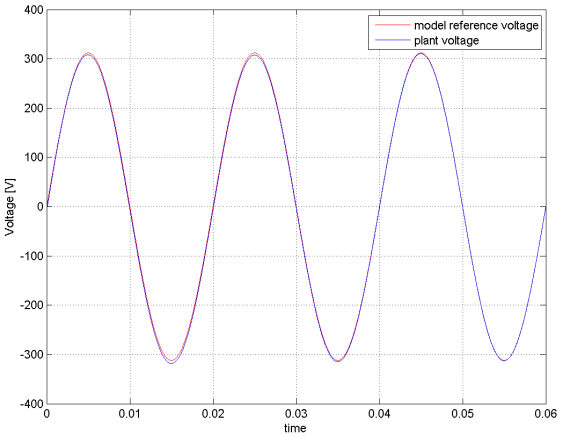

Figure 51: A zoom of the voltage evolution

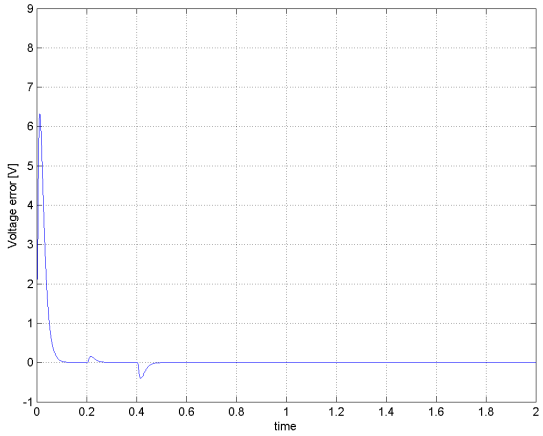

Figure 52: Voltage error dynamic

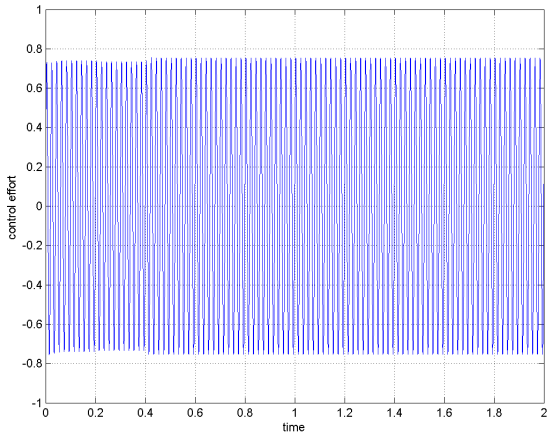

Figure 53: Control effort dynamic

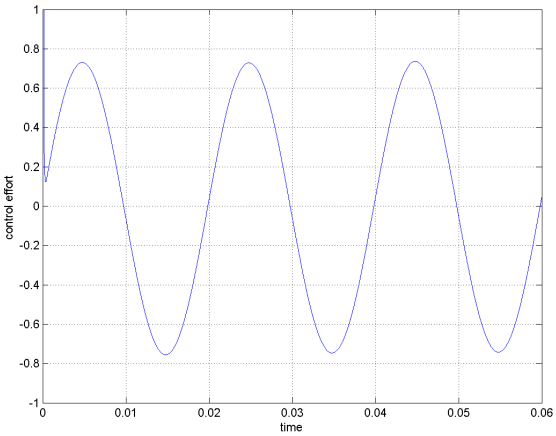

Figure 54: A zoom of the control effort

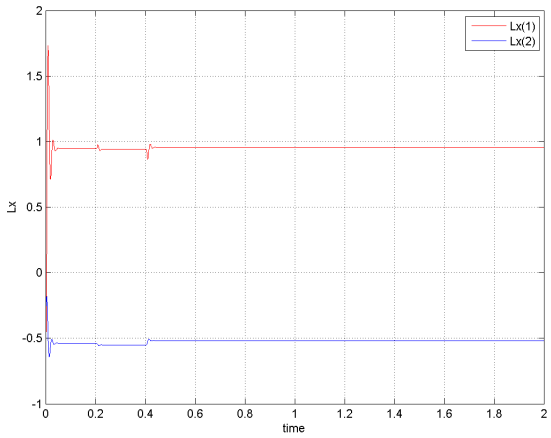

Figure 55: Lx gain dynamics

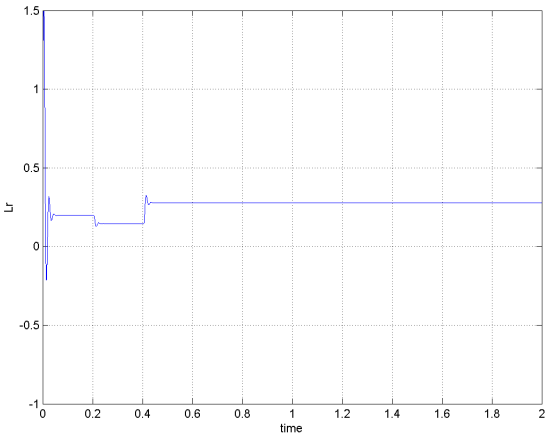

Figure 56: Lr gain evolution

8.2 Nonlinear dynamic model

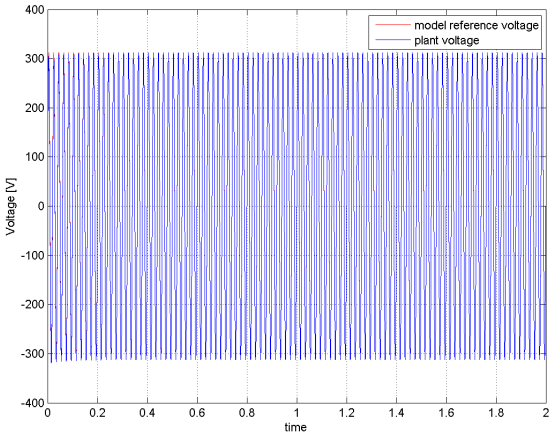

Figure 57: output voltage

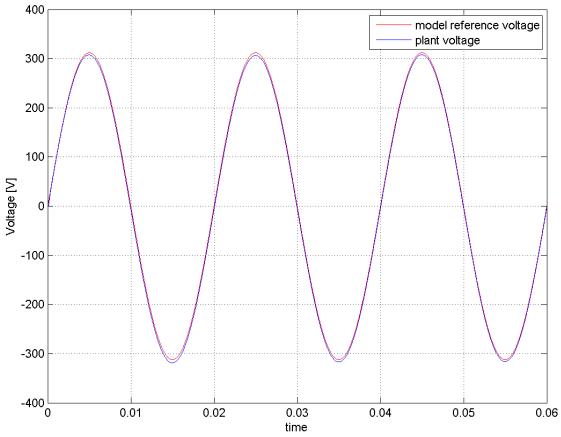

Figure 58: A zoom of the voltage evolution

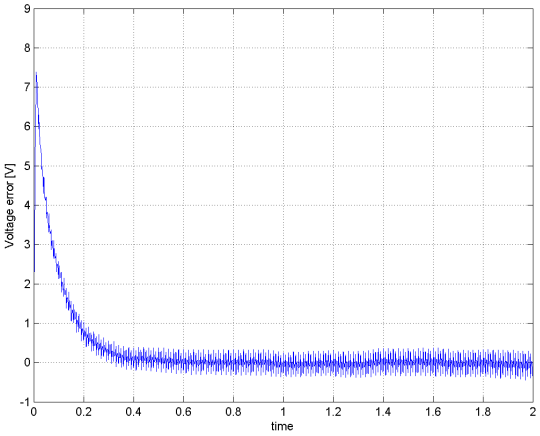

Figure 59: Voltage error dynamic

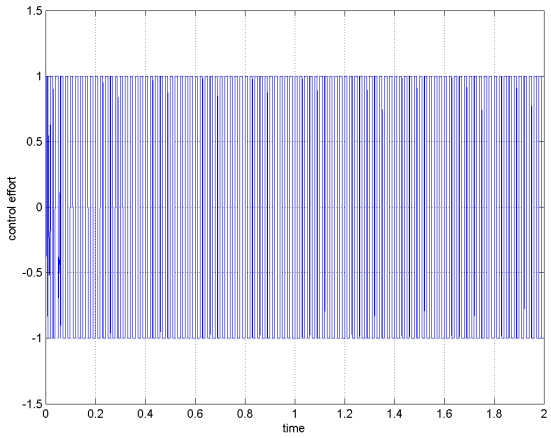

Figure 60: Control effort dynamic

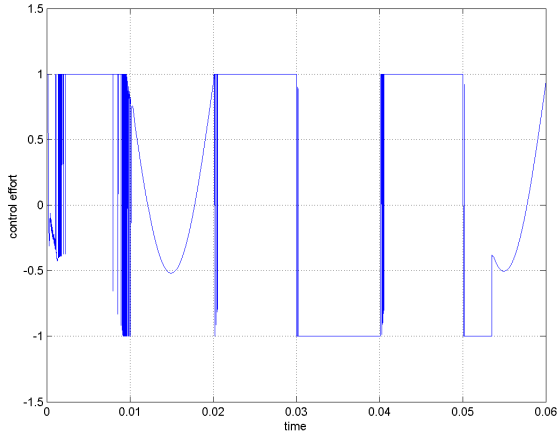

Figure 61: A zoom of the control effort trajectory

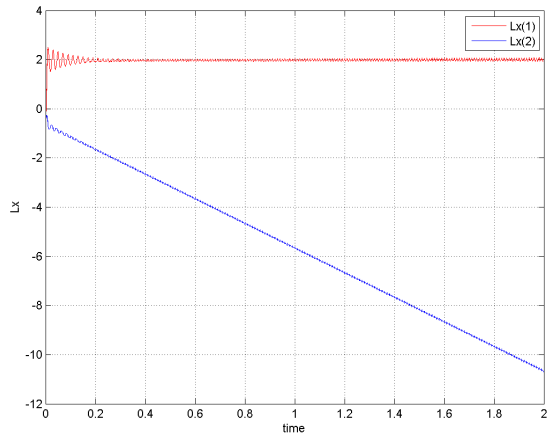

Figure 62: Lx gain dynamics

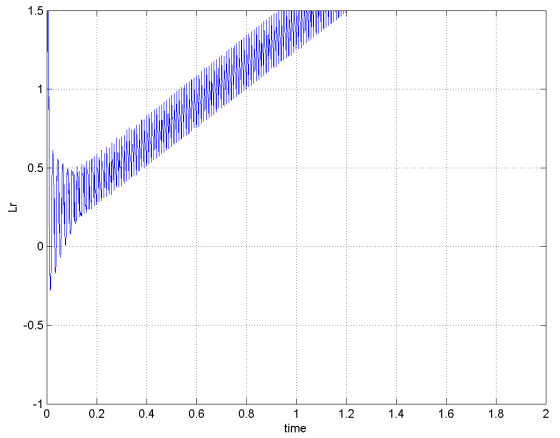

Figure 63: Lr gain evolution

Choosing the N gain in adaptive way:

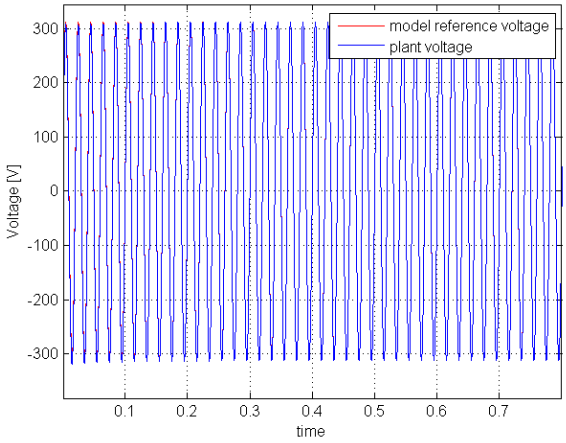

Figure 64: output voltage

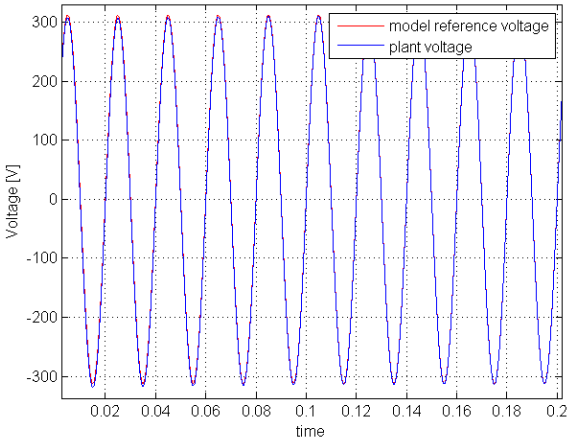

Figure 65: A zoom of the voltage evolution

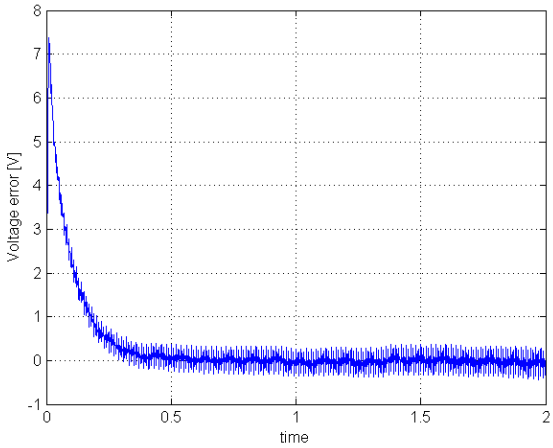

Figure 66: Voltage error dynamic

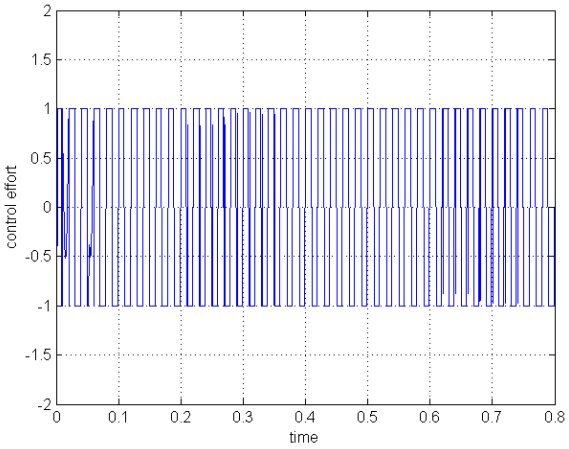

Figure 67: Control effort dynamic

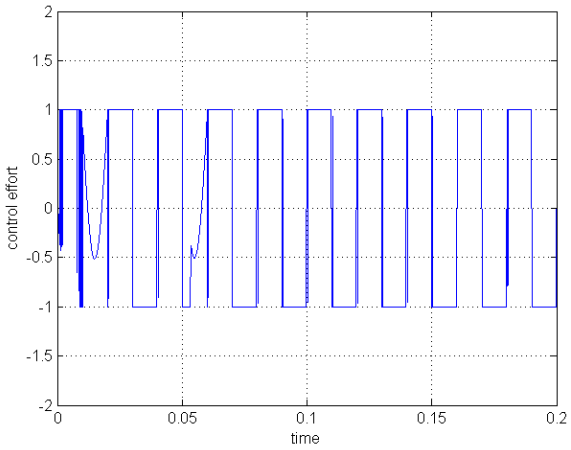

Figure 68: A zoom of the control effort trajectory

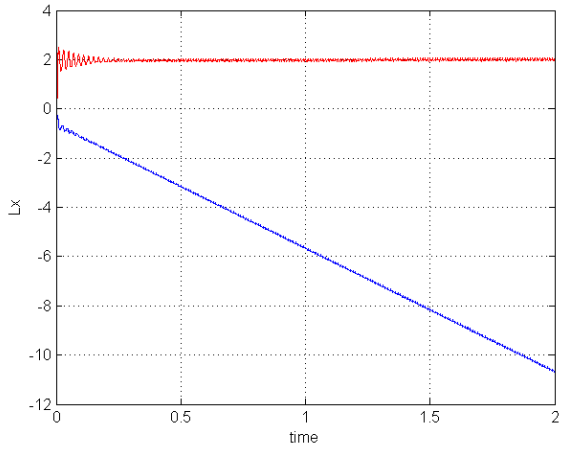

Figure 69: Lx gain dynamics

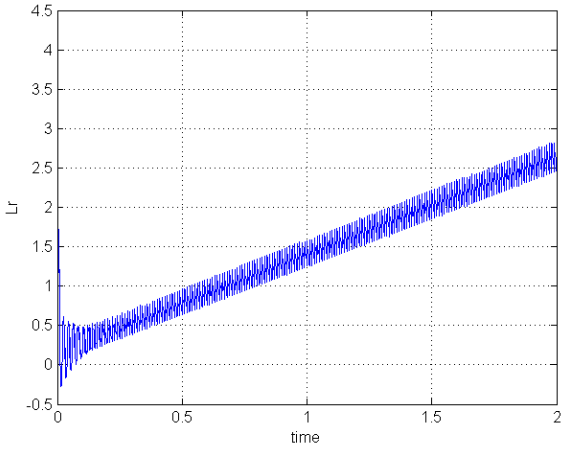

Figure 70: Lr gain evolution

Modeling the sliding action with a continuous law:

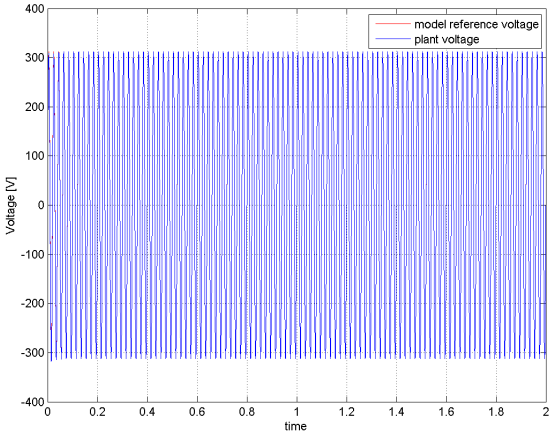

Figure 71: output voltage

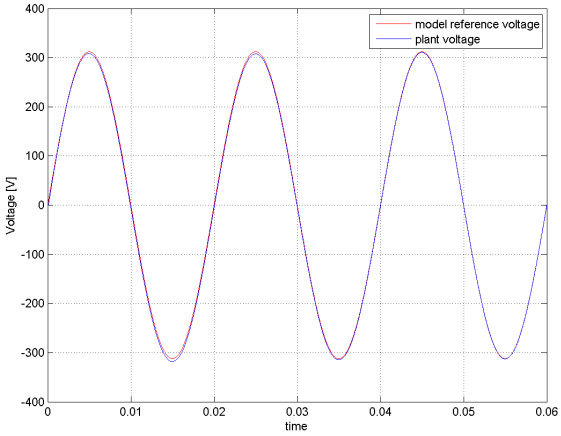

Figure 72: A zoom of the voltage evolution

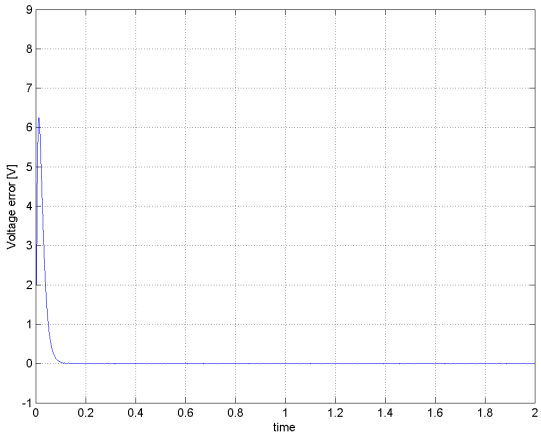

Figure 73: Voltage error dynamic

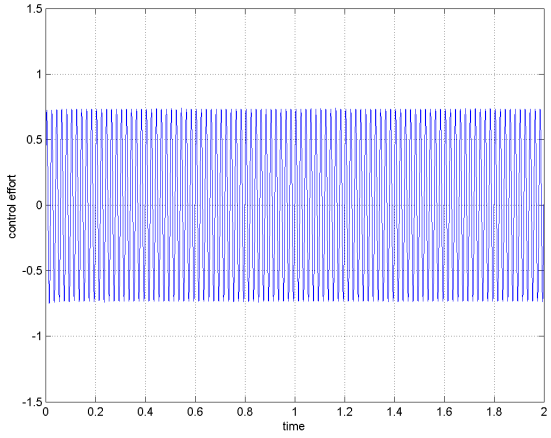

Figure 74: Control effort dynamic

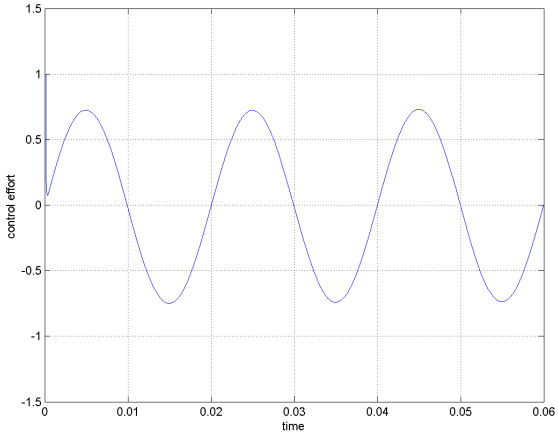

Figure 75: A zoom of the control effort

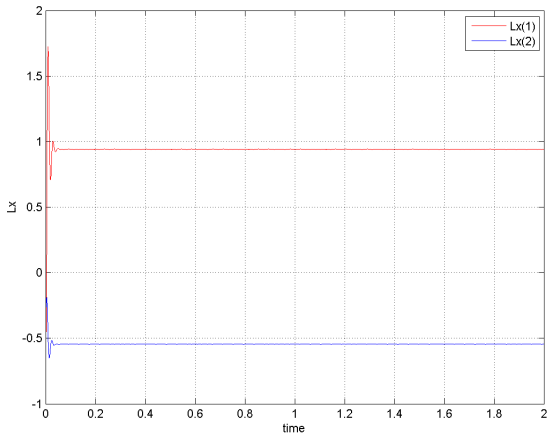

Figure 76: Lx gain dynamics

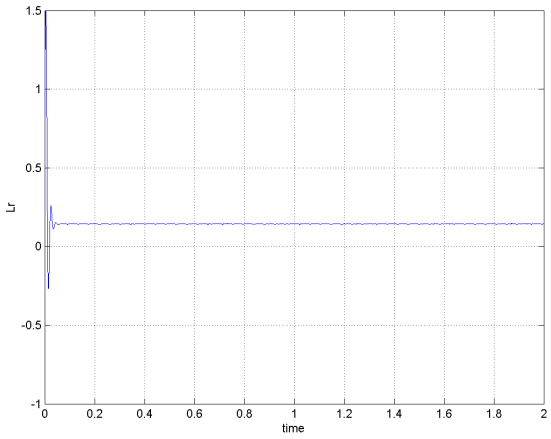

Figure 77: Lr gain evolution

8.3 Results

By comparing the obtained results it's easy to see that in the first solution the systems states error decays smoothly towards a bandwidth $\pm 0.3V$ fig.38 instead of zero, in addition the discontinuous sliding action improves the controller performance but, as expected, the EMCS control input is affected by the chattering introduced by the high frequency switching action and also saturate fig.39 and fig.40.;another problem is the increase of the control gains as shown in fig.41 and fig.42. The difference between the classic and the adaptive is not appreciable in this particular case as depicted in fig.45-49. On the other hand the continuous solution, choosing properly the N gain, seems to significantly reduce the error amplitude fig.52 without introducing any kind of ripple and distorsion on the control action as shown in fig.53 and fig.54 and on control gains fig.55 and fig.56; this seems to be the best solution. For the Nonlinear load the results are almost the same of the linear ones.

9 Closed loop MCS controller with PWM modulation

In this section has been introduced a PWM generator that inject the signal produced by the controller into the plant switches at $20kHz$,in order to make more faithful to reality the simulation, it has been implemented using the MATLAB/SIMULINK toolbox SimPowerSystems.

9.1 Linear model

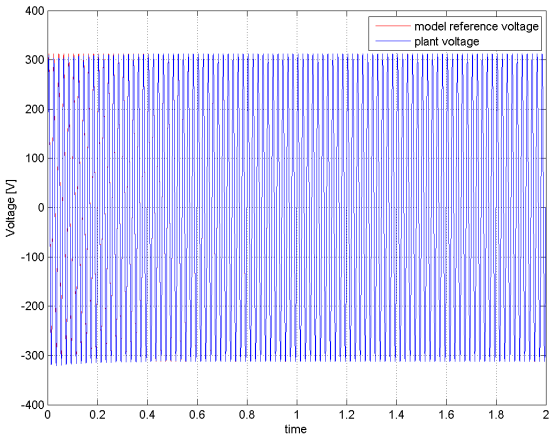

Figure 78: output voltage

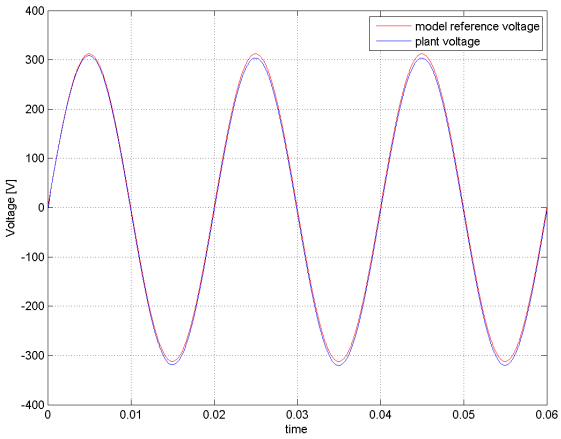

Figure 79: A zoom of the voltage trajectory

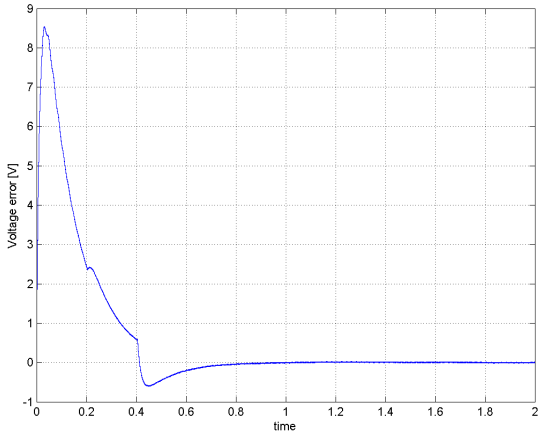

Figure 80: Error dynamic

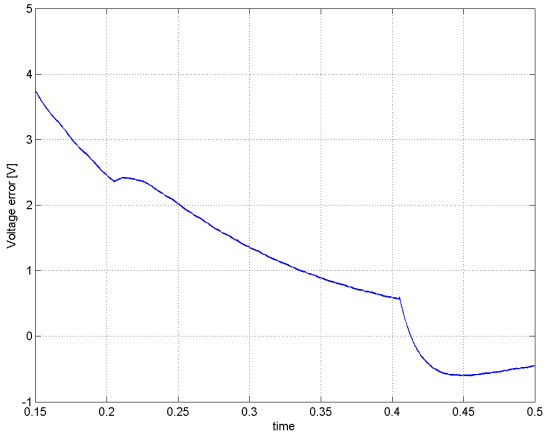

Figure 81: A zoom of the error trajectory

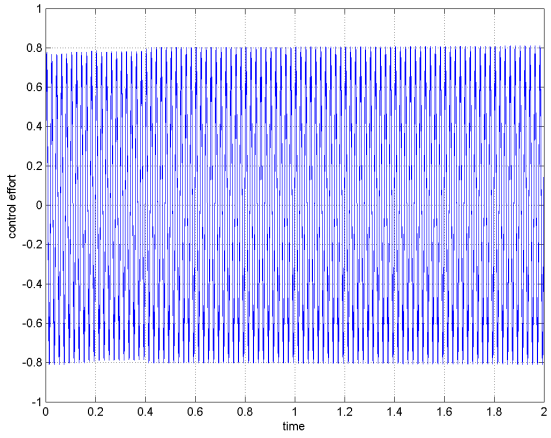

Figure 82: Control effort trajectory

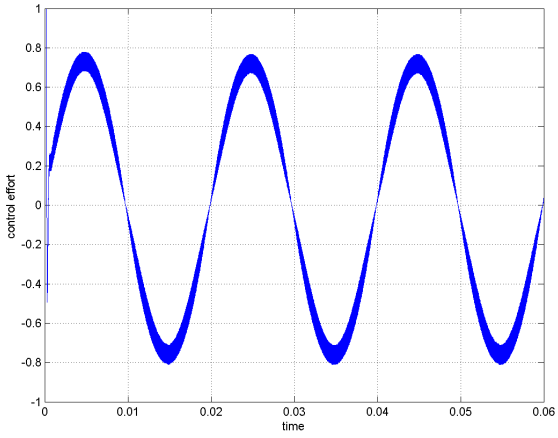

Figure 83: A control effort magnification

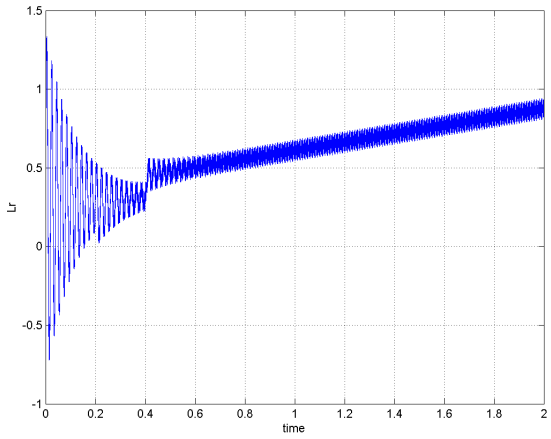

Figure 84: Lr gain trajectory

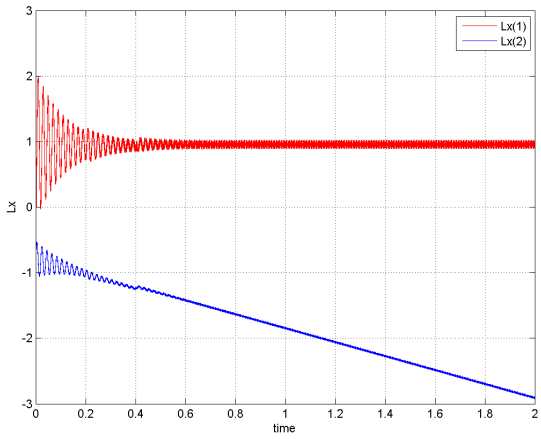

Figure 85: Lx gains evolution

9.1.1 Gain locking and gain bounding

The numerical results shows that the Lx gain increases indefinitely in absolute value.In order to avoid controller memory overflow problems has been implemented a gain locking strategy introducing a correction term $g(t)$ in the integral part of the gain to lock as:

$$L_I = \int (\alpha y(t)x(t) + g(t))\mathrm{d}t$$

$$g(t) = \begin{cases} 0 \quad if \quad L_I \in (L_I^a, L_I^b) \\ -\alpha y(t)x(t) \quad if \quad L_I = L_I^a \\ -\alpha y(t)x(t) \quad if \quad L_I = L_I^b \end{cases}$$

where L_I^a and L_I^b are respectively the lower and the upper bound. This solution can imply a loss of performance for this reason is possible,according with [9] to retain the

favorable dynamics of the gain imposing only a bounding and not a complete locking in the following way:

$$L_I = \int (\alpha y(t)x(t) + g(t))\mathrm{d}t$$

$$g(t) = \begin{cases} 0 \quad if \quad L_I \in (L_I^a, L_I^b) \\ 0 \quad if \quad L_I = L_I^a \quad and \quad \alpha y(t)x(t) \geq 0 \\ 0 \quad if \quad L_I = L_I^b \quad \alpha y(t)x(t) \leq 0 \\ -\alpha y(t)x(t) \quad if \quad \dot{L}_I = 0 \end{cases}$$

where L_I,L_I^a and L_I^b have the same meaning of the previous case.

The upper and lower bound empirically imposed for the gains are:

* $L_{Ir}^b = 5$
* $L_{Ir}^a = -1.5$
* $L_{I1}^b = 2.1$
* $L_{I1}^a = -0.3$
* $L_{I2}^a = 0.5$
* $L_{I2}^b = -2$

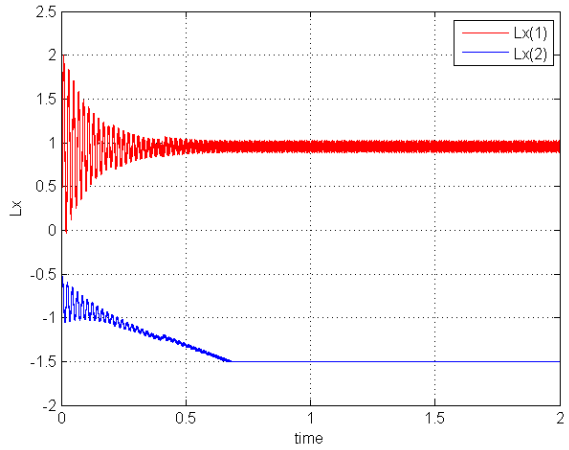

Figure 86: Lx gain locked

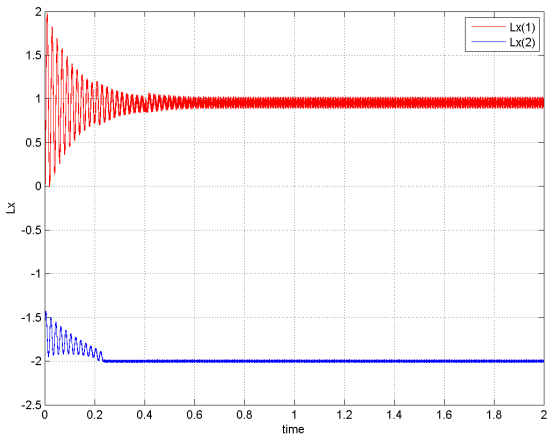

Figure 87: Lx gain bounded

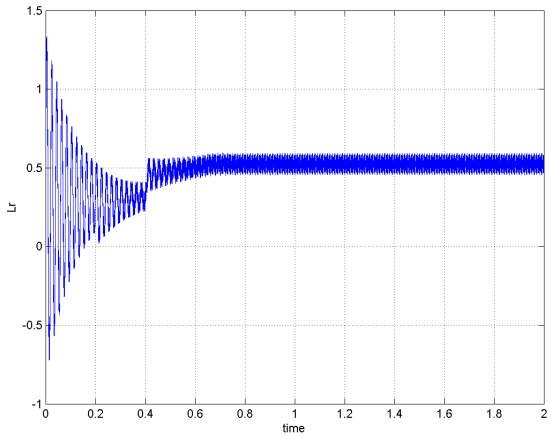

Figure 88: Lr gain locked

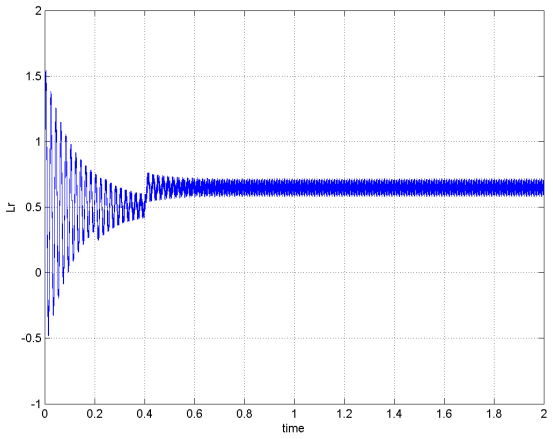

Figure 89: Lr gain bounded

9.2 Nonlinear dynamic model

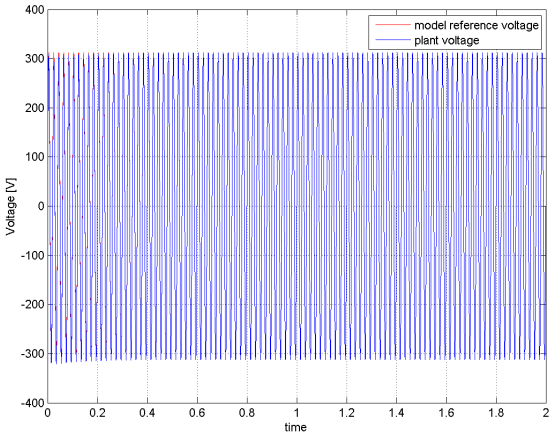

Figure 90: output voltage

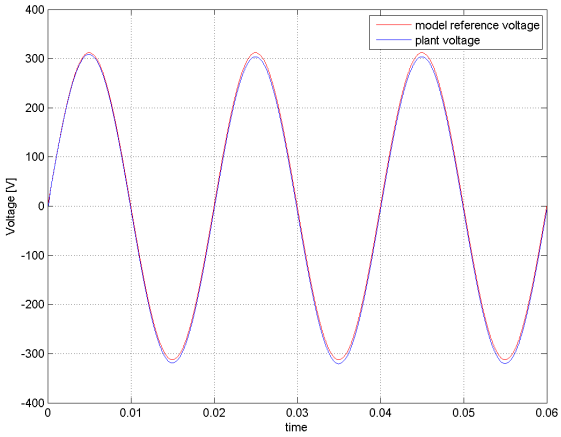

Figure 91: A zoom of the voltage trajectory

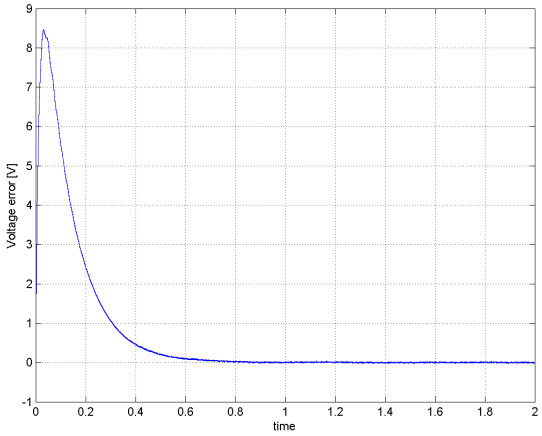

Figure 92: Voltage error dynamic

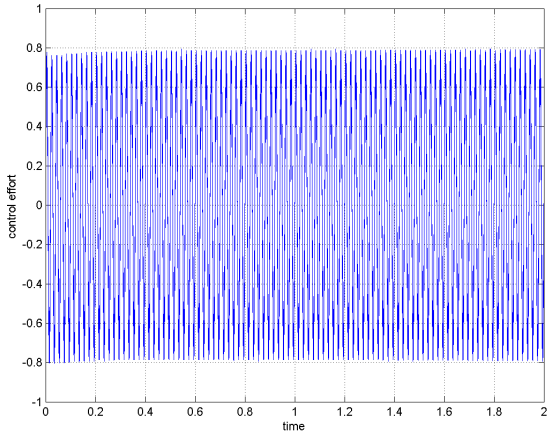

Figure 93: Control effort evolution

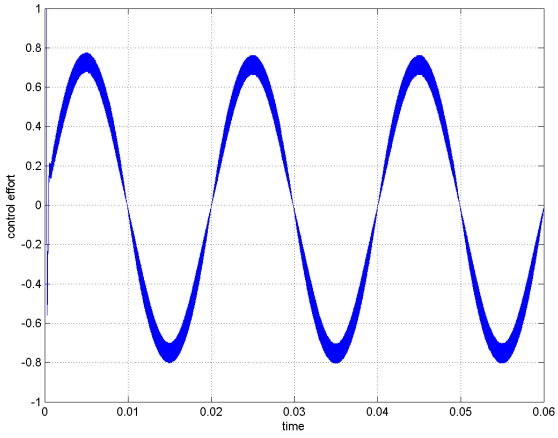

Figure 94: A zooom of control effort transient

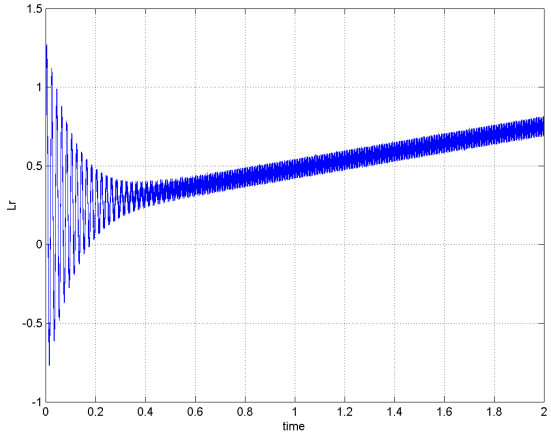

Figure 95: Lr gain trajectory

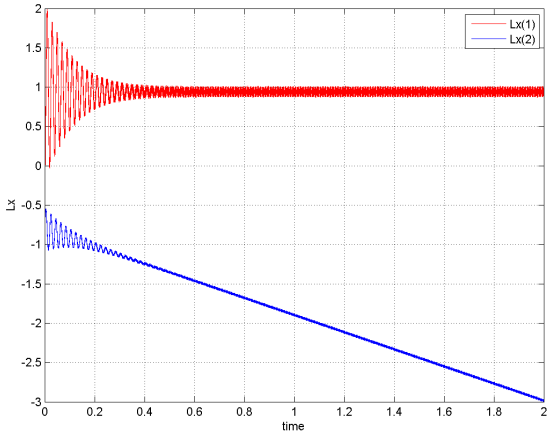

Figure 96: Lx gains evolution

9.2.1 Gain locking and gain bounding

Also for this case had been implemented a gain locking and a gain bounding strategy:

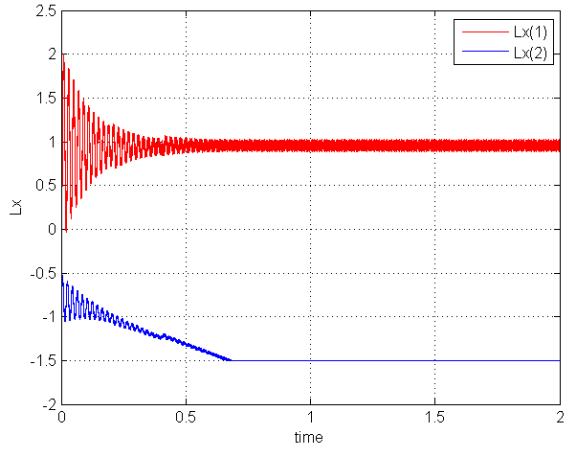

Figure 97: Lx gains locked

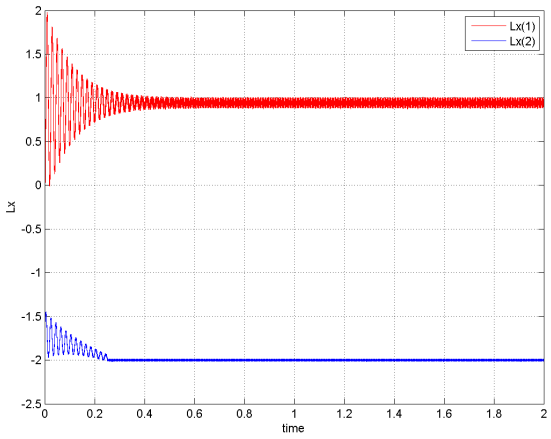

Figure 98: Lx gains bounded

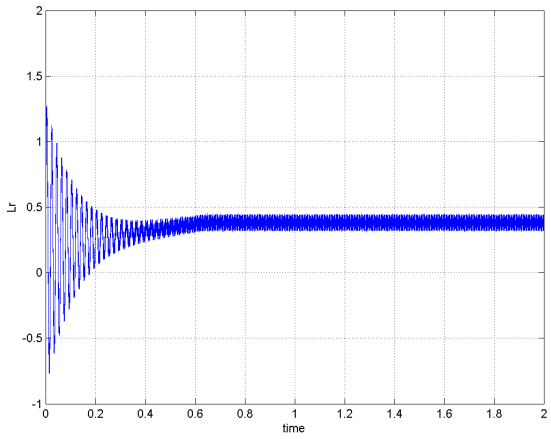

Figure 99: Lr gain locked

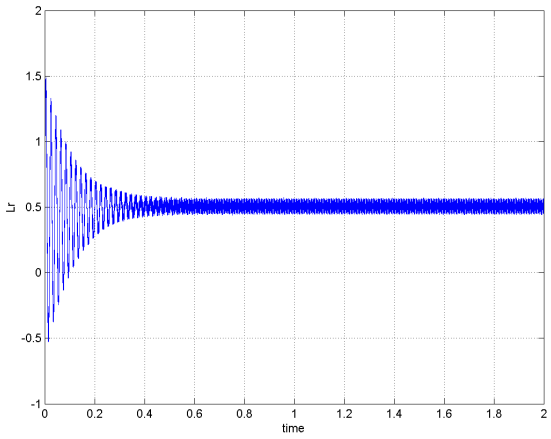

Figure 100: Lr gain bounded

9.3 Results

Observing the output voltage shape in fig.78 it is possible to see a good tracking of the reference signal, in this case the tracking is not perfect, contrarily to previous simulation, as showed in fig. 80 where the maximum error is about 2.5%, the same of the previous case, but it decays to a bandwidth of about $\pm 0.01V$, this ripple is due to the PWM action. In fig.81 it's given a zoom of the error trajectory corresponding to the load jump to evaluate the recovery capabilities of the control. The control effort in this case is not a pure sine but a very good approximation as showed in fig.83. The Lx and Lr gains evolutions are shown in fig.84 e fig.85,notice that in this particular case do not reach a steady-state but grow indefinitely, below are compared the gain locking, fig.86 and fig.88, and the gain bounding, fig.87 and fig.89, solutions. For the Nonlinear load current the results are almost the same as shown from fig.90 to fig.96.

10 Discrete MCS

In the previous sections is proven that the best performance are offered by the EMCS controller, in particular when the sliding action it is modeled by a continuous function, but considering that:

* the improvement is very little compared with the standard MCS
* there is a ripple due to the sliding action
* do not exist a discrete time extended minimal control synthesis theory

In this section the simulations are done with the standard MCS algorithm for comparative purposes.

10.1 Closed loop discrete MCS on linear model

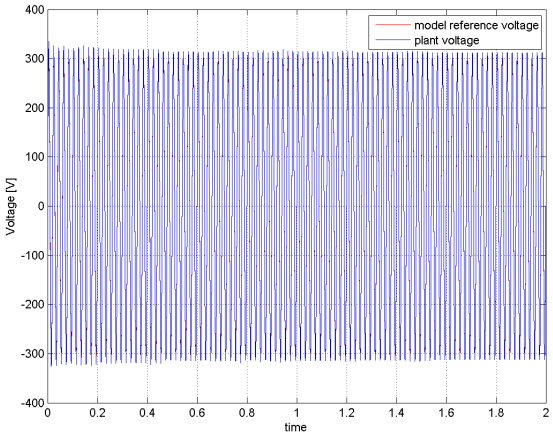

Figure 101: Output voltage

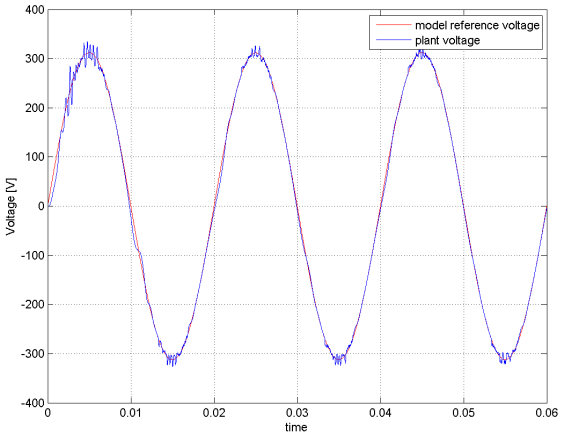

Figure 102: Voltage transient magnification

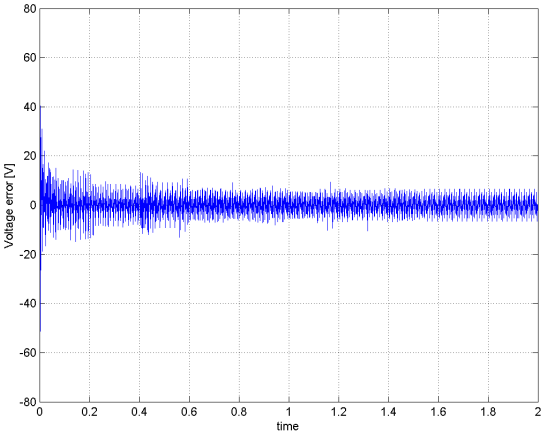

Figure 103: Error trajectory

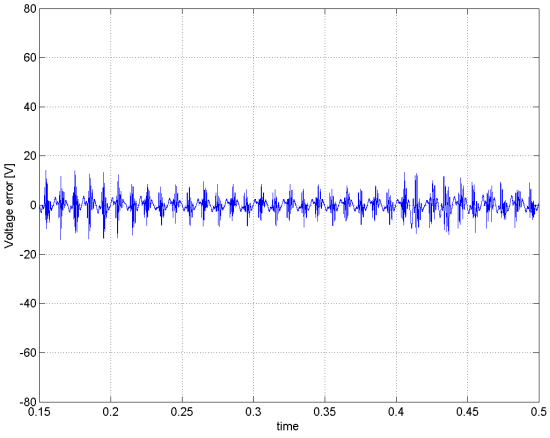

Figure 104: A zoom of the error evolution

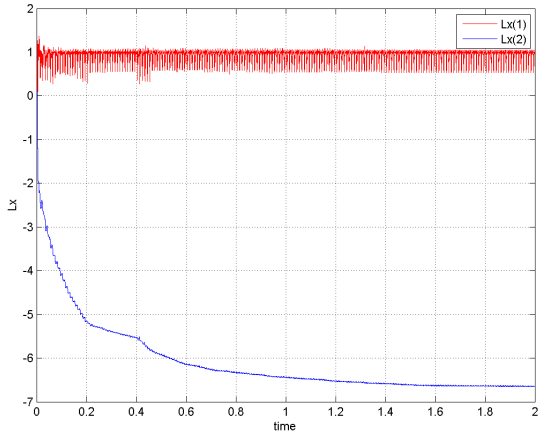

Figure 105: Lx gain trajectory

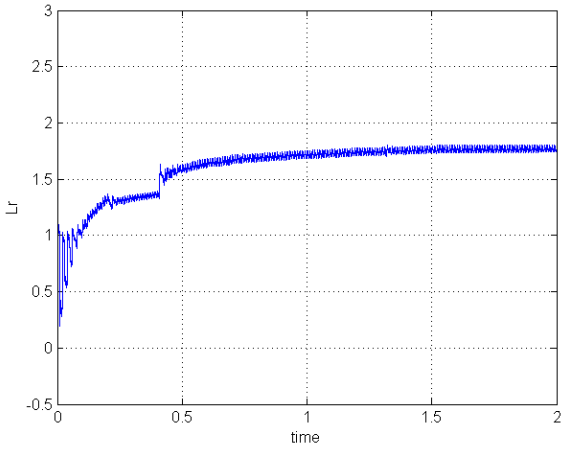

Figure 106: Lr gains evolution

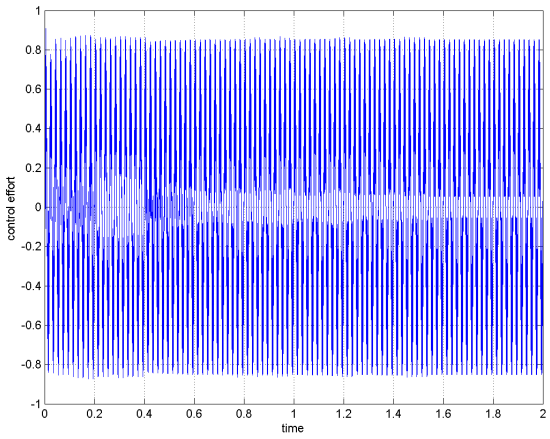

Figure 107: Control effort

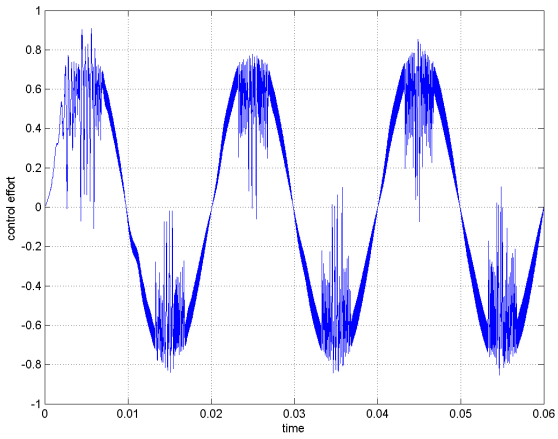

Figure 108: A zoom of the control effort

In fig.102 is shown the output voltage shape, in fig.103 and 104 is depicted the error trajectory, in fig 105 and fig.106 the gains evolution and in fig.107 and fig.108 the control effort all affected by noise.
In order to improve the discrete controller performances is introduced a high frequency filtering action on the current.

10.2 Closed loop discrete MCS on linear model with current filtering action

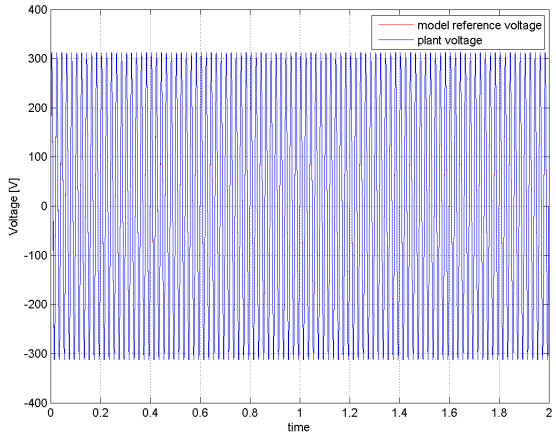

Figure 109: Output voltage

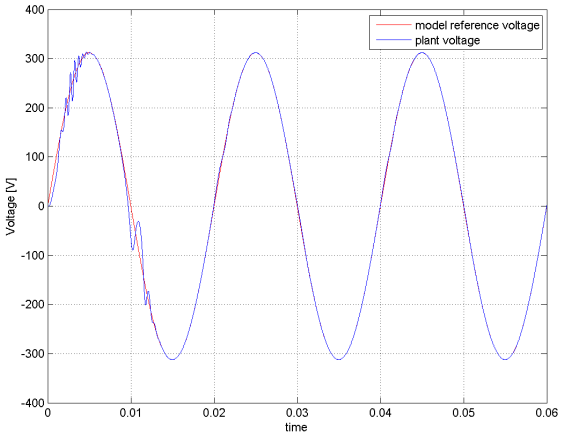

Figure 110: Voltage transient magnification

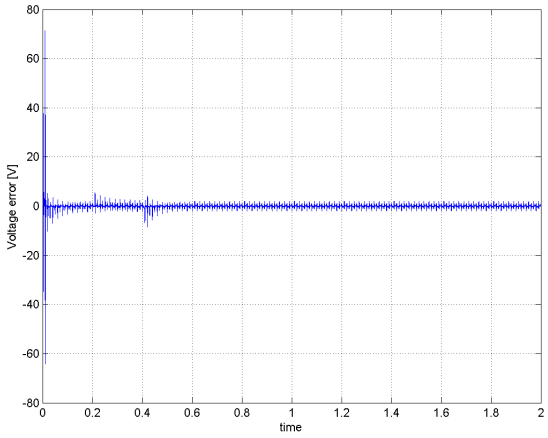

Figure 111: Error trajectory

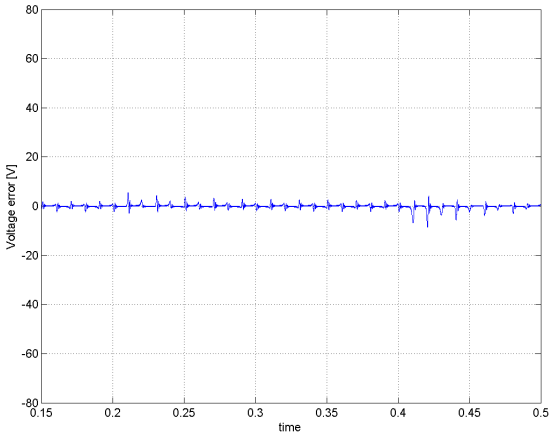

Figure 112: A zoom of the error evolution

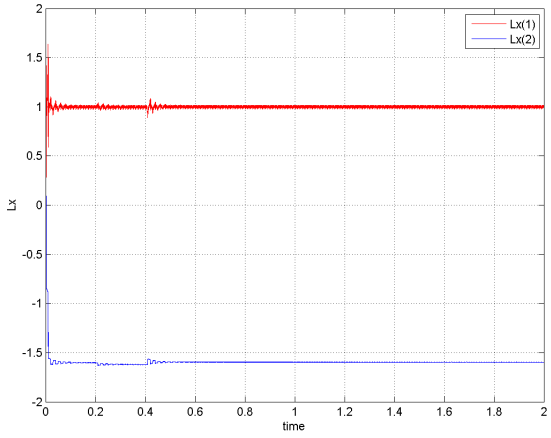

Figure 113: Lx gain trajectory

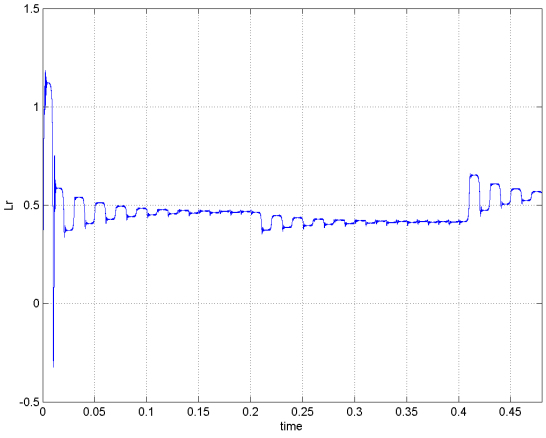

Figure 114: Lr gains evolution

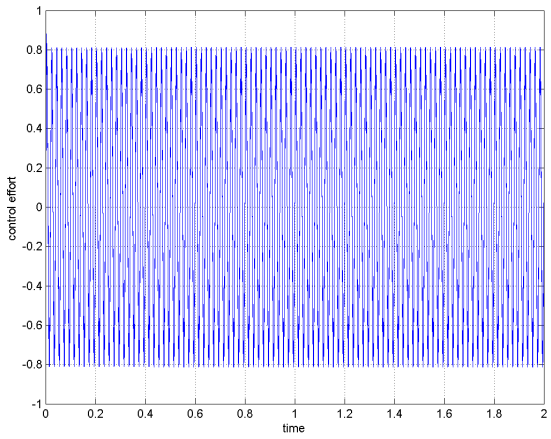

Figure 115: Control effort

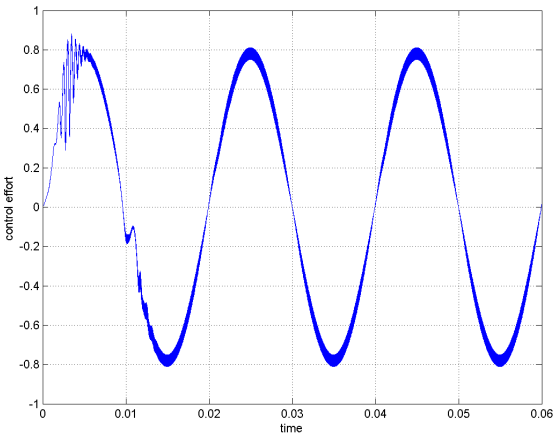

Figure 116: A zoom of the control effort

10.3 Closed loop discrete MCS on nonlinear model with current filtering action

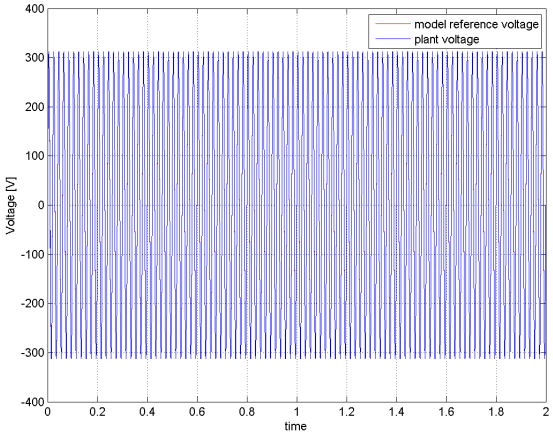

Figure 117: Output voltage

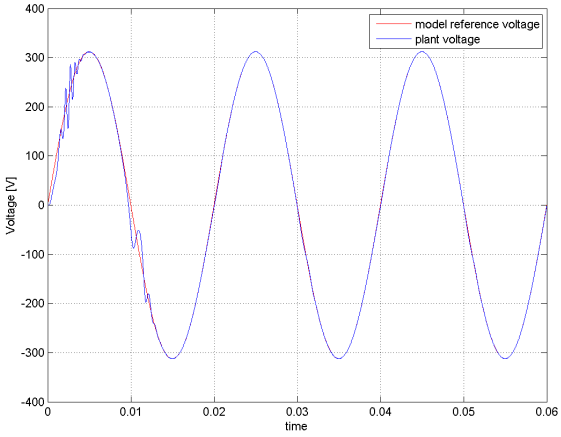

Figure 118: Voltage transient magnification

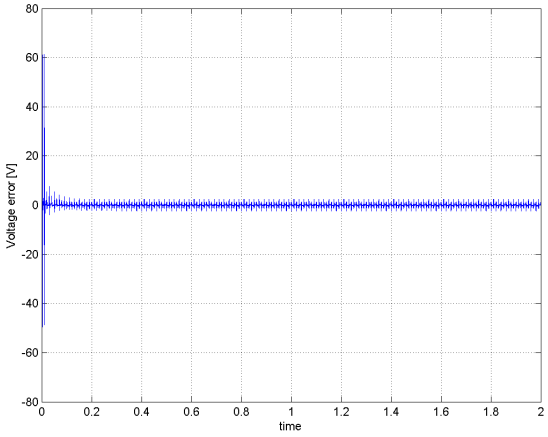

Figure 119: Error trajectory

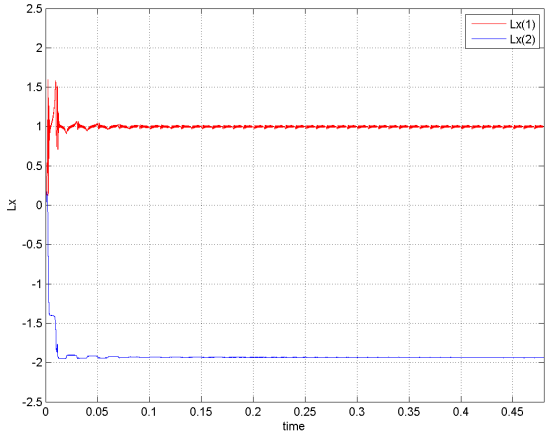

Figure 120: Lx gain trajectory

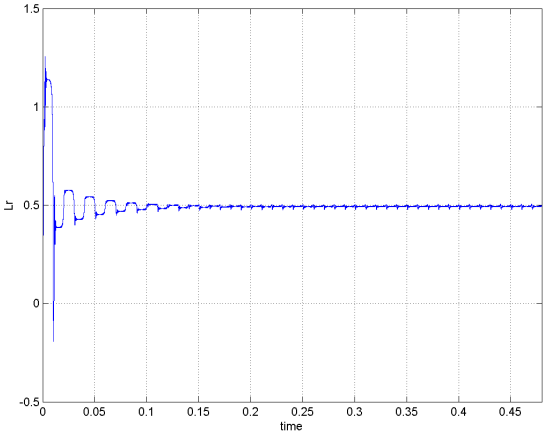

Figure 121: Lr gains evolution

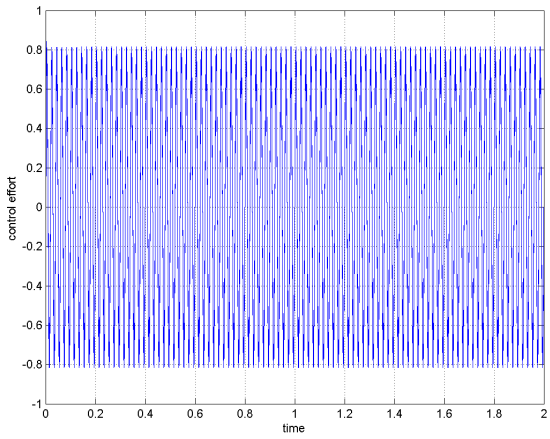

Figure 122: Control effort

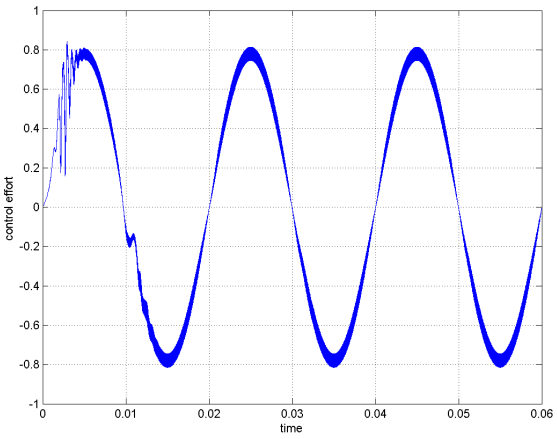

Figure 123: A zoom of the control effort

The upper and lower bound empirically imposed for the gains are:

* $L_{Ir}^b = 0.9$
* $L_{Ir}^a = -0.09$
* $L_{I1}^b = 1.3$
* $L_{I1}^a = -0.1$
* $L_{I2}^a = -1$
* $L_{I2}^b = 0.1$

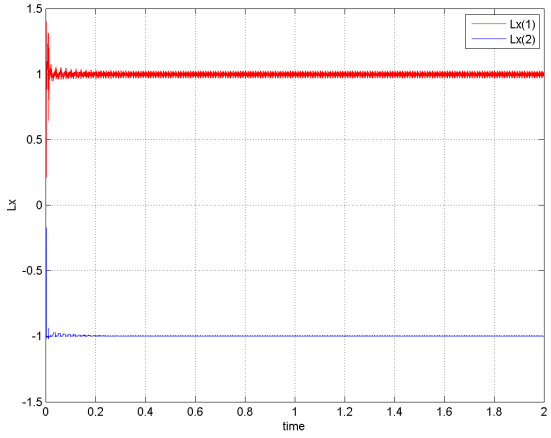

Figure 124: Lx gains bounded

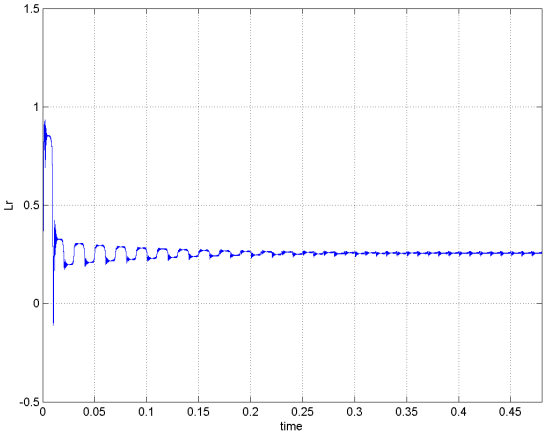

Figure 125: Lr gain bounded

10.4 Results

Fig.109 and fig.110 depicted the output voltage and the reference profile. The tracking error of the overall simulation is depicted in fig.111 a magnification is given in fig.112.Notice the maximum error, as expected, appears in the very first time instants of simulation, when the adaptation is just started than decays quickly to a bandwidth of $\pm 2V$, i.e. a 0.6%, in a very short time. This steady error is mainly due to the finite switching frequency of the PWM Generator. Only when load changes arise the error goes up to$\pm 4V$, i.e.below a $\pm 1.2\%$, witch means an extremely low overshoot for such a large jump of the parameter value.This is in accordance with the reported improvement of the disturbance accommodation capabilities of the MCS controlled systems as time increases due to adaptive gain evolution. In fig 113 and fig.114 are shown the Lx and Lr gain evolution, the response of the adaptive mechanism to the load changes is evident. The control effort is given in fig.115 and fig.116, notice that never saturated, because it is kept within the expected bandwidth ± 1. For the nonlinear load the results are at least the same of the linear case as shown in fig.117-123. To avoid the possibility of overflow errors also in this case has been implemented a gain bounding strategy fig.124 and fig.125.

11 Discrete EMCS

With no theoretical guarantee the sliding continuous term had been discretized with forward Euler's method and implemented only as a try, below are shown the empirical results:

11.1 Discrete EMCS on linear model

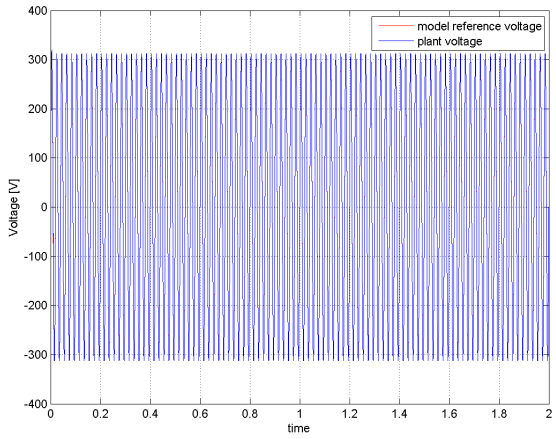

Figure 126: Output voltage

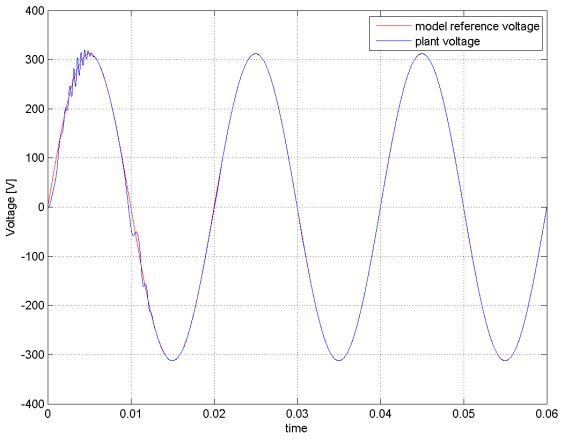

Figure 127: Voltage transient magnification

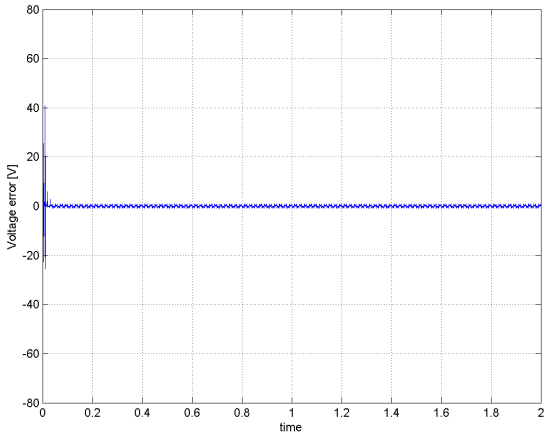

Figure 128: Error trajectory

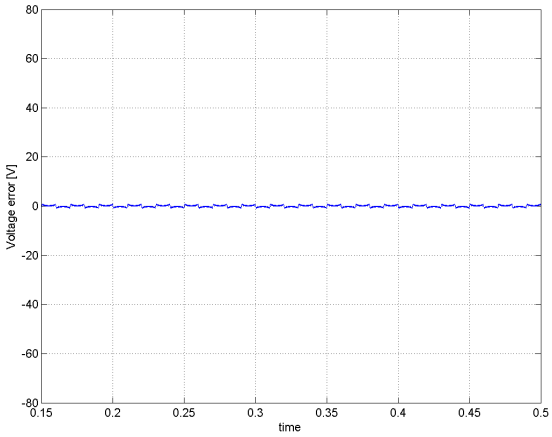

Figure 129: A zoom of the error evolution

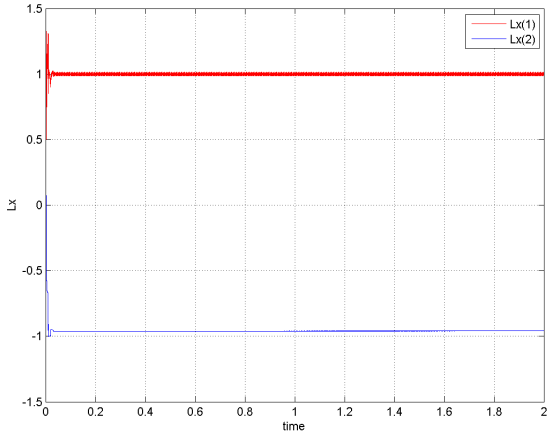

Figure 130: Lx gain trajectory

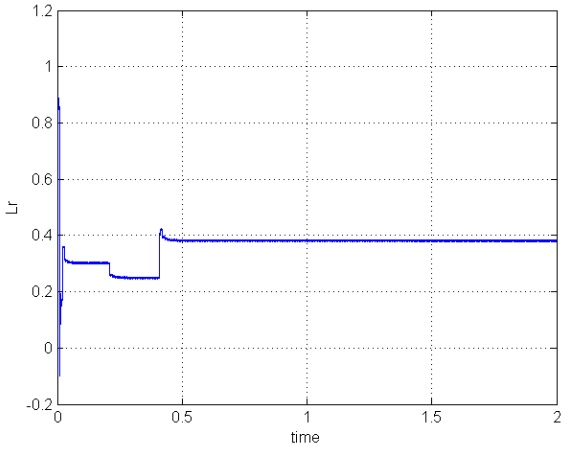

Figure 131: Lr gains evolution

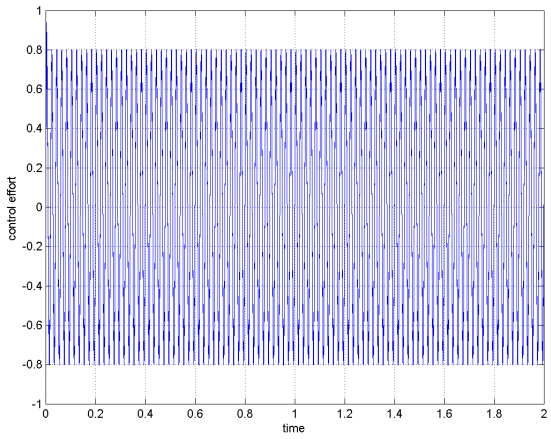

Figure 132: Control effort

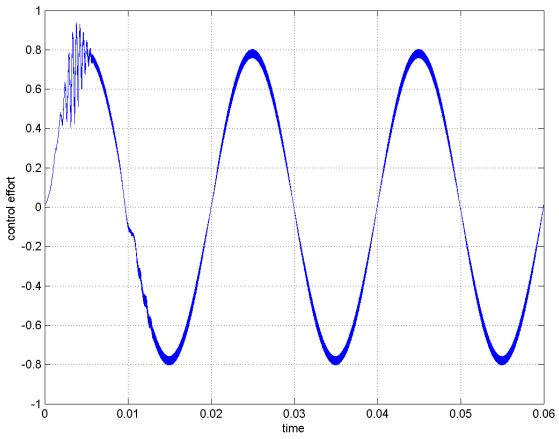

Figure 133: A zoom of the control effort

11.2 Discrete EMCS on nonlinear model

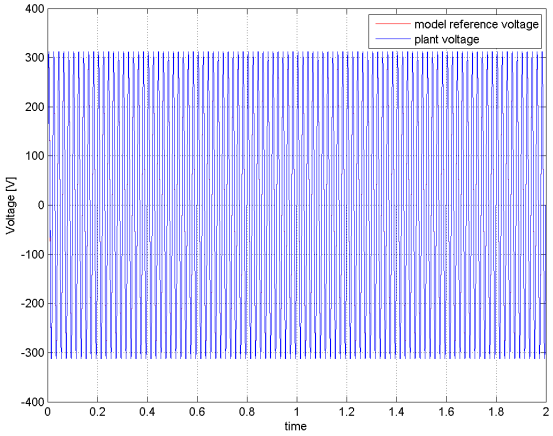

Figure 134: Output voltage

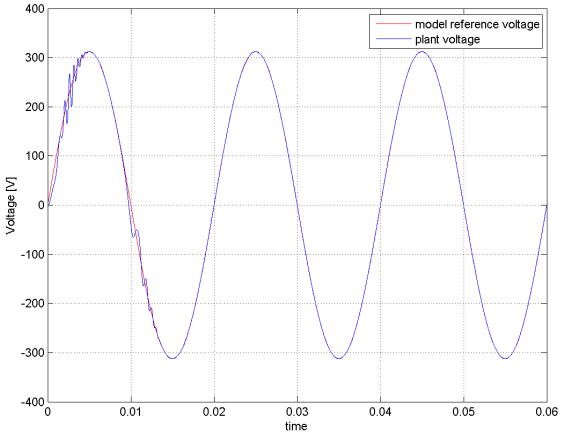

Figure 135: Voltage transient magnification

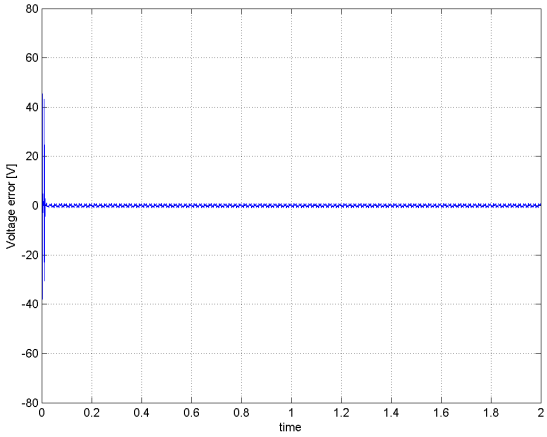

Figure 136: Error trajectory

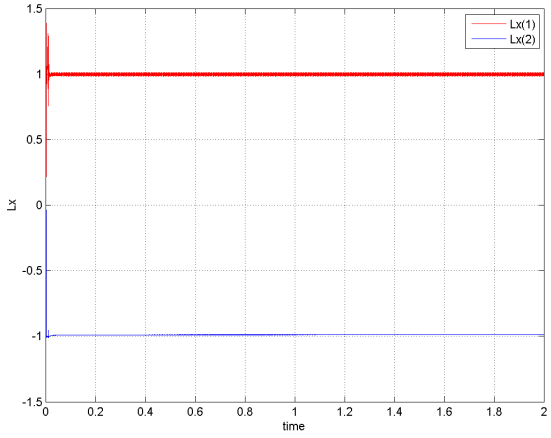

Figure 137: Lx gain trajectory

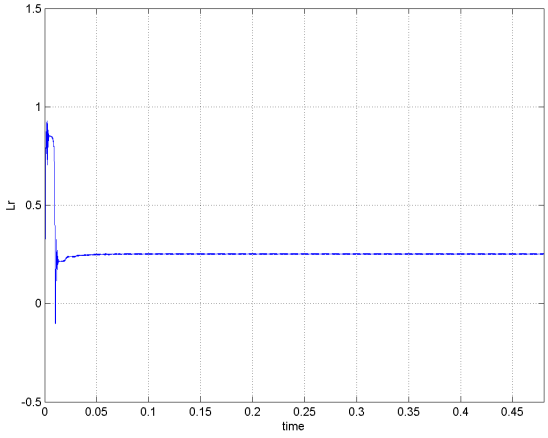

Figure 138: Lr gains evolution

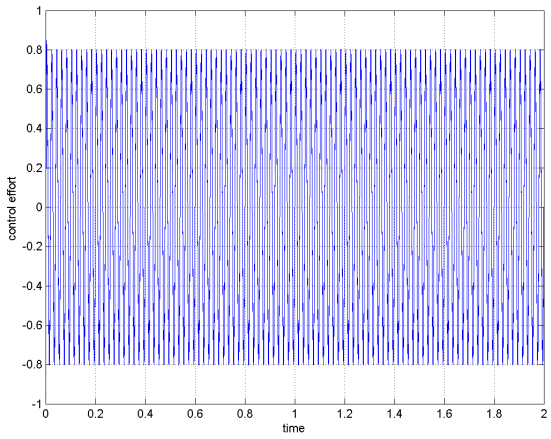

Figure 139: Control effort

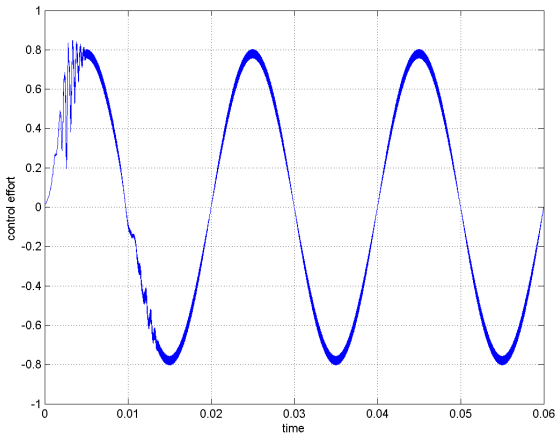

Figure 140: A zoom of the control effort

11.3 Results

The simulation shown that the EMCS retains all the advantages of the MCS controller offering a reduction of the steady error over the 60% to the previous simulation as shown in fig.128 and fig.136.

12 Conclusions

Numerical results showed that the control algorithm, used for the first time on this kind of power converter, offered an excellent closed-loop behavior even though the control signal was injected to the plant by a PWM generator at a realistic frequency. The advantage provided are:

* shorter transients,
* lower steady-state error,
* superior ability to compensate large resistive load jumps without losing performance,
* the good compensation of nonlinear loads.

Concluding the MCS strategy reveals as a promising alternative for controlling this kind of device.

References

[1] A. Salvi, S. Santini, D. Biel and J. M. Olm, Model reference adaptive control of a full-bridge buck inverter with minimal controller synthesis, accepted for presentation in the 52th IEEE conference on Decision and Control, Florence, Italy, 2013.

[2] M. di Bernardo D. P. Stoten, A New Extended Minimal Control Synthesis Algorithm with an Application to the Control Chaotic Systems, Proceedings of the 36th Conference on Decision Control, San Diego, California USA, 1997

[3] D. P. Stoten, H. Benchoubane, The extended minimal controller synthesis algorithm, International Journal of Control, 56:5, 1139-1165, 1992

[4] D. P. Stoten, H. Benchoubane, Empirical studies of an MRAC algorithm with minimal controller synthesis, Internat. J. Control, vol 51, no. 4, pp. 823-849,1990.

[5] D. P. Stoten, H. Benchoubane, Robustness of a minimal controller synthesis algorithm, Internat. J. Control, vol 51, no. 4, pp. 851-860.

[6] D. P. Stoten, The adaptive minimal control synthesis algorithm with integral action, In Proc. 21st, Conf. on Ind. Elec. Control and Inst., Orlando (FLA), pp. 1646-1651, 1995

[7] M. di Bernardo, F. di Gennaro, Olm, J. M.,S. Santini, Discrete-time minimal control synthesis adaptive algorithm., International Journal of Control, Vol. 83, No. 12, 12.2010, p. 2641 - 2657.

[8] Y.D. Landau, Adaptive Control: The Model Reference Approach, Marcel Dekker, Ink., NY,1979.

[9] G. Tao, Adaptive Control of Systems with Nonlinearities,John Wiley Sons, 2003.